Aus dem Lehrstuhl

für Röntgendiagnostik

Prof. Dr. Christian Stroszczynski

Optimizing coronary computed tomography angiography

using a novel deep learning-based algorithm

Inaugural – Dissertation

zur Erlangung des Doktorgrades

der Medizin

der

Fakultät für Medizin

der Universität Regensburg

vorgelegt von

Hendrik Jürgen Heinz Dreesen

2024

Aus dem Lehrstuhl

für Röntgendiagnostik

Prof. Dr. Christian Stroszczynski

Optimizing coronary computed tomography angiography

using a novel deep learning-based algorithm

Inaugural – Dissertation

zur Erlangung des Doktorgrades

der Medizin

der

Fakultät für Medizin

der Universität Regensburg

vorgelegt von

Hendrik Jürgen Heinz Dreesen

2024

Dekan: Prof. Dr. Dirk Hellwig

1. Berichterstatter: Prof. Dr. Christian Stroszczynski

2. Berichterstatter: Prof. Dr. Sabine Fredersdorf-Hahn

Tag der mündlichen Prüfung: 13. Juni 2024

Erklärungen

Die Dissertation wurde angeregt und ihre Ausarbeitung überwacht durch Prof. Dr. Christian Stroszczynski.

Ich erkläre hiermit, dass ich die vorliegende Arbeit ohne unzulässige Hilfe Dritter und ohne Benutzung anderer als der angegebenen Hilfsmittel angefertigt habe. Die aus anderen Quellen direkt oder indirekt übernommenen Daten und Konzepte sind unter Angabe der Quelle gekennzeichnet. Insbesondere habe ich nicht die entgeltliche Hilfe von Vermittlungs- bzw. Beratungsdiensten (Promotionsberater oder andere Personen) in Anspruch genommen. Niemand hat von mir unmittelbar oder mittelbar geldwerte Leistungen für Arbeit erhalten, die im Zusammenhang mit dem Inhalt der vorgelegten Dissertation stehen. Die Arbeit wurde bisher weder im In- noch im Ausland in gleicher oder ähnlicher Form einer anderen Prüfungsbehörde vorgelegt.

_____

Hendrik Dreesen, Nürnberg 12.06.2024

Table of Content

Zusammenfassung:

Hintergrund: Die koronare Computertomographiean-giographie (CCTA) ist ein wesentlicher Bestandteil der Diagnose des chronischen Koronarsyndroms (CCS) bei Patienten mit einer niedrigen bis interme-diären Vortestwahrscheinlichkeit. Minimale techni-sche Anforderung für die CCTA ist eine 64-Zeilen-Multidetektor-CT (64-MDCT), die zwar aufgrund ihrer Verfügbarkeit häufig Anwendung findet jedoch durch ihre begrenzte zeitliche Auflösung und z-Abdeckung anfällig für Bewegungsartefakte ist. In dieser Studie bewerten wir das Potenzial eines auf Deep Learning basierenden Bewegungskorrekturalgorithmus (MCA), um diese Bewegungsartefakte zu eliminie-ren.

Methoden: In dieser Studie wurden 124 mit einer 64-MDCT durchgeführten CCTA-Untersuchungen mit zumindest geringfügigen Bewegungsartefakten aus-gewertet. Die Bilder wurden unter Verwendung eines konventionellen Rekonstruktionsalgorithmus (CA) und eines MCA rekonstruiert. Die Bildqualität (IQ) wurde gemäß einer fünfstufigen Likert-Skala pro

Segment, pro Arterie und pro Patient bewertet und mit potenziell Störfaktoren (Herzfrequenz (HR), intrazyklische HR-Veränderungen (ΔHR), Body mass index (BMI), Alter und Geschlecht) korreliert. Auf statistische Signifikanz wurde mittels Wilcoxon-Vorzeichen-Rang-Test und auf Korrelation mittels Spearman's Rho getestet.

Ergebnisse: Pro Patient nahm der Anteil der CCTA-Untersuchungen mit unzureichender IQ um 5,26% ab, und der mit ausreichender IQ stieg um 9,66% mit MCA. Pro Arterie nahm der Anteil mit unzureichender IQ der rechten Koronararterie (RCA) um 18,18% ab, und der mit ausreichender IQ stieg um 27,27%. Pro Segment nahm der Anteil mit unzureichender IQ in den Segmenten 1 und 2 um 11,51% bzw. 24,78% ab, und der mit ausreichender IQ stieg um 10,62% bzw. 18,58%. Die Gesamtanzahl der Artefakte pro Arterie verringerte sich in der RCA von 3,11 ± 1,65 auf 2,26 ± 1,52. Die Abhängigkeit der IQ der RCA von der HR nahm in Bildern mit MCA-Rekonstruktion zu einer intermediären Korrelation ab.

Zusammenfassung: Der angewandte MCA verbessert die IQ von mit 64-MDCT aufgenommenen Bildern und reduziert den Einfluss der HR auf die IQ, was die Validität von 64-MDCT bei der Diagnose von CCS erhöht.

Abstract:

Background: Coronary computed tomography angiography (CCTA) is an essential part of the diagnosis of chronic coronary syndrome (CCS) in patients with low-to-intermediate pre-test probability. The minimum technical requirement is 64-row multidetector CT (64-MDCT), which is still frequently used, although it is prone to motion artifacts because of its limited temporal resolution and z-coverage. In this study, we evaluate the potential of a deep-learning-based motion correction algorithm (MCA) to eliminate these motion artifacts.

Methods: 124 64-MDCT-acquired CCTA examinations with at least minor motion artifacts were included. Images were reconstructed using a conven-

tional reconstruction (CA) algorithm and an MCA. Image quality (IQ), according to a five-point Likert scale, was evaluated per segment, per artery, and per patient and was correlated with potentially disturbing factors [heart rate (HR), intra-cycle HR changes, BMI, age, and sex]. Comparison was done by Wilcoxon-Signed-Rank test, and correlation by Spearman's Rho.

Results: Per patient, insufficient IQ decreased by 5.26%, and sufficient IQ increased by 9.66% with MCA. Per artery, insufficient IQ of the right coronary artery (RCA) decreased by 18.18%, and sufficient IQ increased by 27.27%. Per segment, insufficient IQ in segments 1 and 2 decreased by 11.51% and 24.78%, respectively, and sufficient IQ increased by 10.62% and 18.58%, respectively. Total artifacts per artery decreased in the RCA from 3.11 ± 1.65 to 2.26 ± 1.52. HR dependence of RCA IQ decreased to intermediate correlation in images with MCA reconstruction.

Conclusion: The applied MCA improves the IQ of 64-MDCT-acquired images and reduces the influence of

HR on IQ, increasing 64-MDCT validity in the diagnosis of CCS.

1 Introduction

Since the introduction of the 64-multidetector computed tomography (MDCT) scanner, computed CT angiography (CCTA) has emerged as a widely accessible and established non-invasive diagnostic tool for assessing chronic coronary syndrome (CCS)[1]. Previous studies have demonstrated the equivalence of CCTA to both non-invasive functional testing and invasive coronary angiography (ICA) in the risk assessment and estimation of major adverse cardiovascular events (MACE) in cases with low to intermediate pre-test probability (PTP)[2-5]. These findings are noteworthy, given that ICA is considered the reference method for CCS evaluation, and makes CCTA appealing as an alternative diagnostic method for low to intermediate-risk patients. Particularly, as ICA is associated with a low incidence of serious procedure-related complications, including major bleeding (0.5-2%), heart attack, stroke, or death (0.1-0.2%)[3,6,7]. Moreover, non-invasive functional tests based on CCTA have also been introduced recently,

including computed tomography perfusion (CTP) and fractional flow reserve CT (FFR$_{CT}$)[8,9]. In this way, CCTA can be used to assess the hemodynamic significance of a coronary stenosis, increasing the accuracy of CCS diagnosis.

In light of these advancements, the European Society of Cardiology (ESC) has revised its guidelines for the diagnosis and treatment of CCS, now recommending CCTA as the primary diagnostic method for CCS in populations with a low to intermediate PTP[10-12]. However, application of CCTA has limitations as image quality (IQ) can be compromised due to factors such as extensive coronary calcification, the patient's inability to cooperate with breath-hold commands, significant obesity, and a high and variable heart rate (HR and HRv)[13]. Especially, false-positive results due to HR- and HRv-related motion artifacts present a challenge for CCTA, given the small diameter (1-5 mm) of the coronary arteries and a displacement of up to 1 cm during the cardiac cycle[14-16].

Strategies to mitigate the impact of motion artifacts on IQ and interpretability involve both hardware and software approaches. Hardware improvements primarily focus on increasing temporal resolution by reducing gantry rotation time, applying half-scan rotation, and utilizing high-pitch imaging. The introduction of dual-source (DSCT) and MDCT is considered to have the most profound impact on CCTA applicability, as it significantly increases temporal resolution, allowing for the capture of images of the entire heart during one heart cycle[17-20]. Additionally, the effect of cardiac motion can be further reduced by applying prospective electrocardiographic (ECG)-gated axial ("step-and-shoot scan" [PGI]) or retrospective ECG-gated helical (RGH) acquisition to select the most quiescent cardiac phase for imaging, typically the end-systolic and mid-diastolic phase[15,21]. During image reconstruction, RGH merges data from multiple volume blocks acquired during different cardiac cycles within a defined cardiac phase, effectively eliminating motion artifacts at low and constant HR. However, despite efforts such

as ECG-guided tube current modulation and low tube voltage scanning, RGH is associated with a relatively high effective dose due to constant image acquisition[22]. In contrast, PGI-guided acquisition is triggered by a predefined cardiac phase based on the ECG signal (regularly during the R-R interval), minimizing the effective dose compared to RGH[23]. Unfortunately, this makes PGI more dependent on a constantly regular and low HR for accurate acquisition.

Since an optimal HR cannot be guaranteed, HR control is regularly administered through rate-limiting drugs like beta-blockers or ivabradine[20,24]. Sublingual nitroglycerine is also often employed to dilate coronary arteries, enhancing IQ[25]. However, optimal imaging conditions remain challenging in certain situations, such as HRv in cardiac arrhythmias or high HR in patients insensitive to beta-blockers or with contraindications[26,27].

Software-based solutions in the form of motion correction algorithms (MCA) provide an effective remedy for non-diagnostic images plagued by motion artifacts. Currently, there are two vendor-specific

MCA available in the market. SnapShot Freeze (SSF) 1 (GE Healthcare, Waukasha, WI, USA) is primarily designed for CCTA, and its updated version, SSF2 (GE Healthcare), can be employed not only for CCTA but also for whole heart imaging, such as the assessment of the aortic annulus in transcatheter aortic valve replacement[28,29]. These algorithms generate images from data captured during adjacent cardiac phases within a single cardiac cycle, occurring 60 milliseconds before and after a predefined target phase. This approach minimizes beat-to-beat inconsistencies, heart period variations, or gantry period resonance points that could potentially affect the reconstruction. Motion artifacts are corrected by determining the current vessel position and estimating the motion path and velocity in the predefined target phase, enabling adaptive correction[28,29].

In several phantom models, SSF1 has been described as a useful tool for motion correction, especially at high HR. It has been shown that SSF1 in combination with dual-energy CT (DECT) and 256-

MDCT can improve image quality and diagnostic accuracy even further[30-32]. In addition, SSF1 itself was used as the basis for further software-based improvement in the accuracy of vessel and stenosis diameters through the use of CT number calibrated diameters [33].

In clinical settings, the application of SSF1 has improved IQ and interpretability in both 64- and 256-detector row CTs[34-37]. Importantly, motion correction with SSF1 has been demonstrated to be independent of HR and HRv in most studies, although some highlight the necessity of sufficient HR control to optimize IQ in the presence of SSF1[38-42]. Additionally, SSF1 has been effective in mitigating image distortions related to body mass index (BMI), such as photon starvation, scatter, and truncation artifacts[43,44]. Therefore, SSF1 is widely regarded as a valuable tool for supporting CCTA in CCS diagnosis and the evaluation of external devices, including stents and coronary artery bypass grafts (CABG)[45-49].

Furthermore, SSF1 has illustrated a reciprocal benefit, not only improving hardware but also benefiting from it. So, the combination of motion correction by SSF1 with DECT has led to further improvements. DECT, characterized by rapid switching between low and high tube potentials, facilitates the reconstruction of monochromatic images. This enhances the contrast of the intracoronary lumen, improving the tracking performance of SSF1. DECT also attenuates blooming and radiation hardening effects associated with excessive calcification, further boosting the effectiveness of SSF1[50,51]. Equally significant, SSF1 serves as a useful complement to PGI, preserving good IQ even at high HR. This allows the application of PGI at higher HR or HRv, resulting in a lower overall effective dose[36,40].

In 2019, SSF2, a further development of SSF1, was introduced. Preliminary literature suggests that the positive effects of SSF2 on IQ are even more profound compared to its predecessor[16]. However, it's important to note that both MCA, SSF1

and SSF2, are vendor-specific and applicable only to specific CT scanners.

Recognizing the clinical utility of MCA in mitigating motion artifacts, there is ongoing exploration of approaches to develop more widely applicable, non-vendor-specific MCA using various technical strategies[52].

Lossau et al. (2019)[53] classified four MCA-based approaches for motion estimation and correction: *registration-based, metric-based, partial angle reconstruction (PAR)-based,* and *image-based approaches*. The registration-based approach, akin to SSF technology, utilizes 3-D/3-D registered filtered back projections (FBP). The core principle involves calculating a 4-dimensional motion vector field (MVF) from two corresponding points of a reference and a target heart phase. The resulting MVF is employed to warp the target phases with respect to the reference phase, achieving a motionless reconstruction. Image data is collected during the most quiescent cardiac phase using ECG-guided acquisition. Despite effectively eliminating motion artifacts, registration-based

methods are associated with a high effective dose due to an extended acquisition period[54-57].

Rohkohl et al. (2013)[58] introduced a metrics-based approach that applies motion artifact metrics (MAM), such as entropy and positivity, to 3-D/3-D FBP for identifying and quantifying motion artifacts. Image reconstructions are iteratively adjusted until motion artifacts reach a minimum. However, metric-based image enhancement is constrained to low and regular HR, limiting its clinical applicability.

PAR-based methods emerge as a promising solution to increase temporal resolution at high HR while minimizing the effective dose. PAR are created by dividing short scan FBP into as many angular segments as possible, reconstructing these segments separately in an angular range much smaller than the short scan range. Although PAR suffer from limited viewing angle artifacts, each PAR is endowed with a very high temporal resolution of 5-10ms, depending on the gantry rotation time. This enables PAR to be utilized for accurate motion estimation and correction[59-62].

Several methods have been proposed to apply PAR in motion correction. Kim et al. (2015)[60] utilized two conjugated PAR images 180° apart to determine the MVF through non-rigid registration. The calculated MVF was then used to warp the PAR with respect to a predefined centered target phase of 90°, obtaining a motion-corrected FBP. Building on this, Kim et al. (2018) developed a motion estimation and correction model to calculate and compensate for motion artifacts in whole-heart images. They estimated 3D MVF based on two orthogonal PAR images, further processing them to 4D MVF, assuming linear motion. These 4D MVF were refined by applying a *metric-based* method to correct inaccuracies due to linear motion estimation, proposing a highly effective MCA[63,64]. However, the reconstruction time for a whole heart image was 35 minutes in this trial, making this approach less suitable for clinical practice[64]. Hahn et al. (2016)[61] also applied PAR, using a single short scan FBP for image data acquisition. Subsequently, the image data were divided into small volumes, utilized for the creation of PAR and a dense

MVF. The MVF were calculated based on a cost function minimizing entropy as a measure of motion artifacts. PAR were employed as a quasi-static representation of the coronary arteries. For motion correction, a central sub-angle image was defined as the reference phase. The remaining sub-angle images were warped by MVF with respect to the reference phase and added to obtain a motion-free image. This *PAR-based* MCA, referred to as partial angle motion correction (PAMoCo), was tested by Hahn et al. (2017) on both a phantom model and real patient data. In this setting, PAMoCo reduced motion artifacts almost independently of HR and cardiac phase. Furthermore, the effective dose exposure was significantly reduced by using a short scan protocol. Nevertheless, PAMoCo still required a computation time for each artery of 10-15 minutes, comparable to Kim et al. (2018)[64,65].

To expedite computation time, *image-based* motion correction has been introduced using deep learning-based MCA, such as Convolutional Neural

Networks (CNN). CNN can be directly applied to reconstructed images without the need for raw data[66]. Notably, Generative Adversarial Networks (GAN) have emerged as prominent examples, comprising a generator and a discriminator CNN. The generator is trained to detect and correct motion artifacts by converting motion-distorted images into motion-free images, with a motion-free target image serving as the ground truth. The discriminator classifies generated motion-free images as real or fake, initiating an iterative learning process until the ground truth and artificial image are indistinguishable. Although initial results of GAN are promising, clinical data are scarce, and computational power requirements remain high[52,67-69].

Apart from GAN, other deep learning-based approaches utilizing CNN have recently been proposed. Lossau et al. (2019)[70] predicted coronary artery motion by applying a new deep-learning MCA called CoMPACT, based on the detection of motion artifact features. For MCA training, they introduced a

deep-learning model that artificially generates motion-disturbed images by computing and inversely applying synthetic MVF. These artificial motion-disturbed images are then used to train algorithms that calculate MVF in terms of motion artifact features. Subsequently, the generated MVF are inserted into an iterative motion correction pipeline to incrementally improve the IQ of real FBP[53]. Although CoMPACT has shown remarkable results in motion correction, its clinical applicability cannot yet be fully assessed due to limited real patient data.

Maier et al. (2021)[62] recently introduced Deep PAMoCo, another *image-based* deep learning MCA. Deep PAMoCo is based on PAMoCo presented by Hahn et al. (2017)[65] and, thus, on Partial Angle Motion Correction (PAMoCo). However, unlike Hahn et al. (2017)[65], Maier et al. (2021)[62] optimized the MVF computation using a deep neural network (DNN) rather than a *metric-based* model. The network was designed to detect motion artifact features and thereby estimate MVF coordinates for ultimately all PAR. For

MCA training, motion-disturbed images were synthetically generated and divided into PAR, serving as input to the motion correction network. The success of the motion correction network was evaluated by comparing the results with the exact motion trajectory used to implement the motion artifacts. The most efficient network was then compared to standard reconstruction and conventional PAMoCo in a small set of real-patient CCTA scans. In these experiments, the reconstruction by Deep PAMoCo was superior to both standard reconstruction and conventional PAMoCo. However, larger clinical studies for Deep PAMoCo with real patient data are still lacking. The aim of this study was to investigate the effect of Deep PAMoCo on CCTA IQ and interpretability with a standard single-source 64-MDCT and to evaluate its impact on IQ affected by mean HR, ΔHR, BMI, gender, and age to assess potential clinical applicability.

2 Materials and Methods

2.1 Image data, algorithm, and CT-scanning

124 CCTA data sets of consecutive patients scanned with the same CT system and the same CT protocol were retrieved from the Picture Archiving and Communication System and included in this study. The clinical indication for CCTA was according to clinical guidelines [71]. Original image data were anonymized, and patients are not identifiable. Consecutive patient data in which at least one vascular segment was affected by motion artifacts were selected for the evaluation with the MCA and a conventional reconstruction algorithm (CA). Since *Deep PAMoCo* is applied to already reconstructed image data, no raw data is required. *Deep PAMoCo* can, therefore, be used on different CT systems without any problems.

The scanning protocol included calcium-scoring, test-bolus-tracking, and CCTA. CCTA imaging

was performed using a 64-MDCT (Siemens Definition 64, Siemens Healthineers, Erlangen, Germany) with a gantry rotation time of 0.33 seconds, a collimation of 64x0.6mm, an automatic, weight-adjusted tube voltage between 100-120kVp, and automatic exposure control. Acquisition was performed with PGI. PGI was performed at a maximum HR ≤80 beats per minute (bpm) during an R-R interval of 60-80% in diastole (average 68%). Low-dose calcium-scoring was performed before CCTA to estimate the patient's calcium load. A calcium score of 1000 was considered the upper limit for CCTA. Patients with a calcium score >1000 were referred to the catheter laboratory. CCTA was performed by trained staff. Beta-blockers were administered orally or i.v. if HR was ≥65bpm after checking contraindications. Sublingual nitroglycerine was administered 2-3 minutes before the examination. For the examination, patients were placed in the supine position, head first. The field of view (FOV) was estimated considering the size of the heart (approximately from 2cm below the carina to the lower edge of the apex cordis). Contrast medium
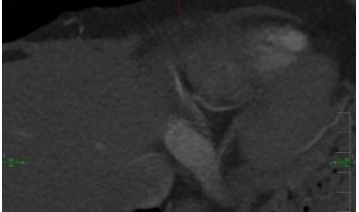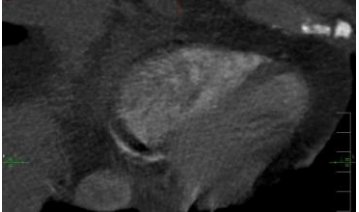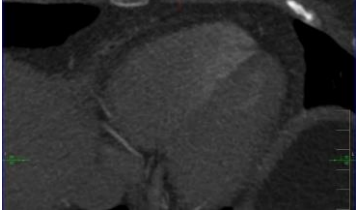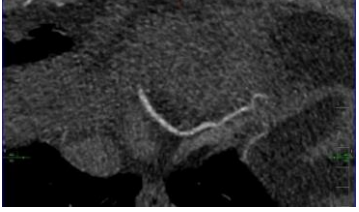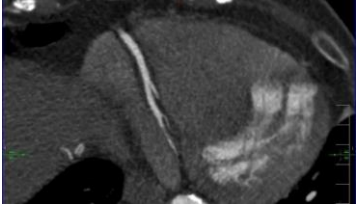
Likert Score description

| 1	Unacceptable: image is not diagnostic due to massive motion artifacts	
2	Below average: image is suboptimal and not diagnostic due to severe motion artifacts	
3	Average: image is readable and diagnostic, slight to moderate motion artifacts are apparent	
4	Above average: image has good IQ; slight motion artifacts are apparent	
5	Excellent: image is perfectly readable; no artifacts are apparent	

Table 1 Likert scale description
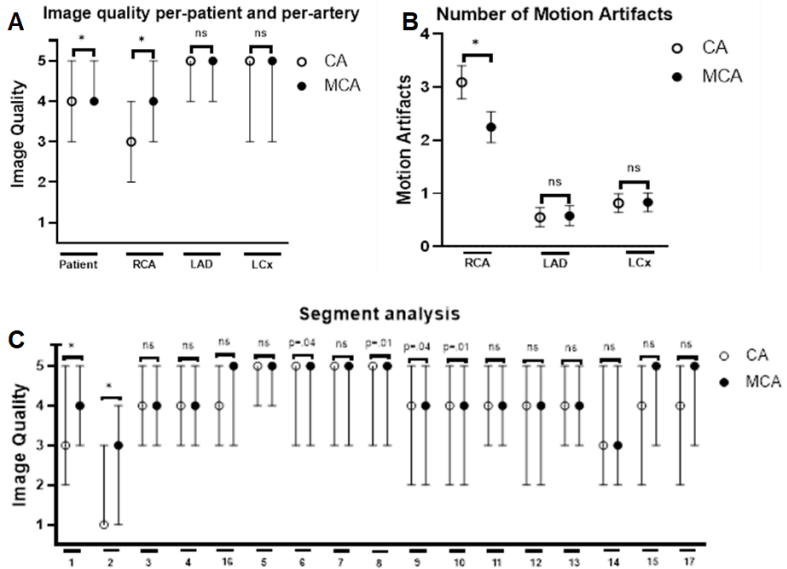
Figure 1 (A) Median and interquartile range (IQR) of image quality per-patient and per-artery with CA and MCA due to a five-point Likert scale. Significance is marked with an asterisk. (B) Mean ±SD of motion artifacts per-artery. Significance is marked with an asterisk. (C) Median and interquartile range (IQR) of image quality per-segment with CA and MCA due to a five-point Likert scale. Significance is marked with an asterisk.

(CM; Solutrast 370, Bracco, Milan, Italy) was administered via an antecubital intravenous line at a flow rate of 6ml/s followed by 30ml of saline at the same flow rate. Body mass index (BMI), age, sex, mean

Study population			
Total (n)	124		
Male/female	59	55	
	Mean	**Range**	**±SD**
Mean age (years)	59,49	21-95	12,53
Mean BMI (kg/m²)	27,58	18,9-43,03	5,21
Mean HR (bpm)	63,92	43-133	11,88
Mean ΔHR (bpm)	7,14	0-105	14,16

Table 2 Study population

HR, and intra-cycle HR changes (ΔHR) were registered.

2.2 Image quality assessment

Images were evaluated by a radiology resident trained for the evaluation of CCTA images. IQ was assessed per segment, per artery (right coronary artery = RCA, left anterior descending artery = LAD, left circumflex artery = LCx), and per patient. Per segment assessment was performed in regard to the Society of Cardiovascular Computed Tomography-

guidelines for the interpretation and reporting of CCTA[72] using a 17-segment approach. A minimal vessel diameter of 2mm was chosen for quality evaluation. IQ was determined using a 5-point Likert scale in terms of image evaluability. The 5-point Likert scale provides accurate information on IQ without being overwhelming. Evaluability was determined based on image readability and the amount of motion artifacts according to previous studies [51]: 1 = unacceptable; 2 = below average; 3 = average; 4 = above average; 5 = excellent (Table 1). The total amount of motion artifacts was assessed by counting the motion artifacts per artery (RCA, LAD, LCx) by identifying typical patterns of motion artifacts as "crescents," "tails," and "horns" (Supp. Fig. 1). MCA-inserted artifacts were assessed by identifying typical patterns as "steps" or vessel "duplications" (Supp. Fig. 2).

2.3 Literature Review

The focus of the literature review was on technical, pharmacological, and software-based methods

for optimizing CCTA and reducing motion artifacts. Systematic literature review was conducted using the online medical literature database 'PubMed.'

The search term employed was 'Coronary computed tomography angiography' in conjunction with the connector "AND" along with 'Motion correction algorithm,' 'motion artifact reduction,' and 'Deep learning-based algorithm.' After entering the respective search terms, the search results were restricted to sources in German and English. In this manner, on 'PubMed,' 55 sources were found for the combination 'Coronary computed tomography angiography AND motion correction algorithm,' 79 for 'Coronary computed tomography angiography AND motion artifact re-duction,' and 53 for 'Coronary computed tomography angiography AND deep learning-based algorithm.' These sources were then assessed for their relevance to this work. The thematic focus of each publication should be on the application of motion correction algorithms to improve the image quality and interpretability of CCTA images. With this focus,

the collected sources were evaluated for their suita-
bility for this work based on their titles and abstracts.
If the thematic focus of the publication appeared suit-
able, the source was obtained in full text, and its con-
tent checked. Literature that was deemed un-suitable
during any part of this evaluation process was ex-
cluded from further processing. Using these gath-
ered publications, an extensive forward and back-
ward search for additional publications was con-
ducted. The goal was to collect sources that investi-
gate the requirements and challenges of CCTA and
both hardware- and software-based methods for re-
ducing motion artifacts in CCTA. Emphasis was
placed on current devel-opments, technical back-
grounds, as well as application results in phantom
models and based on patient data. 'PubMed' was
also utilized for this forward and backward search.

2.4 Statistics

	Motion Artifacts				MCA inserted Artifacts
	CA (Mean)	±SD	MCA (Mean)	±SD	n
RCA	3,11	1,65	2,26	1,52	11
LAD	0,55	0,98	0,58	1,02	0
LCx	0,81	0,94	0,83	0,94	0

Table 3 Mean ±SD of motion artifacts and total number (n) of MCA inserted artifacts per-artery.

Statistical analysis was carried out with JASP team (2022). JASP (version 0.16.4) [computer software]. Continuous variables are expressed as mean ± standard deviation (SD). The central tendency of non-dichotomous categorical variables is expressed as median and percentage. Significance was tested using paired samples tests. A one-tailed p-value of <0.01 is considered to indicate statistical significance in IQ assessment. IQ between the CA and the MCA was compared using the Wilcoxon-Signed-Rank test for ordinal variables. Rank-Biserial correlation was chosen as the effect size measurement. Normality of continuous data was assessed by applying the Shapiro-Wilk test. As continuous data were not normally distributed, the non-parametric Wilcoxon-Signed-Rank test and Rank-Biserial correlation were applied. Correlation analysis between BMI, age, sex,
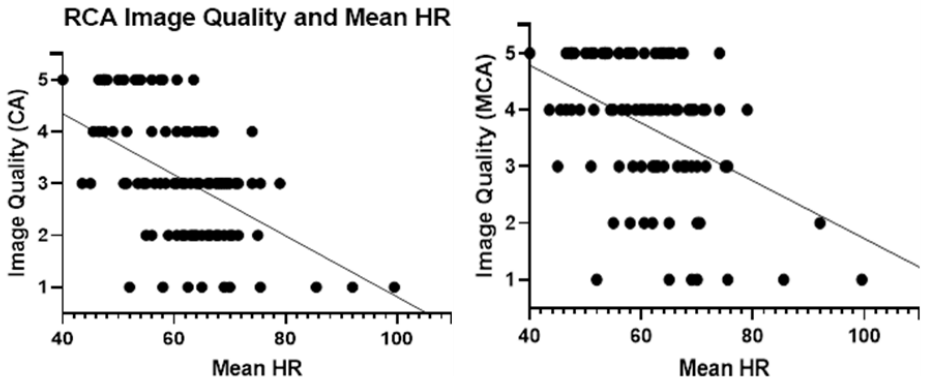
Figure 1 Correlation RCA image quality and mean HR. 0.1=weak correlation, 0.3= moderate correlation, 0.5= strong correlation.

mean HR, and ΔHR and IQ was performed using Spearman's Rho. A two-tailed p-value of <0.01 is considered to indicate statistical significance. Graphs were created using GraphPad Prism, Prism 9 for Windows 64-bit, version 9.5.1 (733), January 26, 2023, tables were created using Microsoft® Excel® 2019 MSO (Version 2303 Build 16.0.16227.20202) 64 Bit.

3 Results

CCTA data sets of 124 patients were evaluated (Table 2). Of these, eleven data sets were excluded due

to severe stack transition, vessel calcifications, and medical devices (stents and pacemakers) producing massive artifacts. BMI was missing in 20 patients; sex, age, ΔHR, and mean HR in nine patients. IQ of 114 patients, 333 arteries, and 3019 segments was evaluated (Figure 2 and 3; Supp. Table 1). Per patient, unacceptable or below-average images decreased from 9.65% to 4.39%, and above-average or excellent images increased from 67.54% to 77.2%. Per artery, the RCA improved significantly. Here, the percentage of unacceptable or below-average images decreased from 36.36% to 18.18%, and above-average or excellent images increased from 31.82% to 59.09%. Per segment, RCA segments 1 and 2 benefited from the MCA. Unacceptable or below-average images decreased from 33.63% to 22.12% and from 71.68% to 46.9%, respectively, while above-average or excellent images increased from 44.25% to 54.87% and from 19.47% to 38.05%, respectively. The total number of artifacts was determined per artery (Figure 4; Supp. Table 2). We observed a decrease in motion artifacts from 3.11 ±

1.65 to 2.26 ± 1.52 in the RCA. There was no significant decrease in motion artifacts in the LAD or LCx. In 11 out of 3019 segments, the IQ deteriorated due to MCA-inserted artifacts, especially in RCA segments 1 and 3. These artifacts mostly resembled vessel "duplications" or "steps ". The correlation between IQ and BMI, age, mean HR, ΔHR, and sex was tested per artery using Spearman's Rho (Figure 5; Supp. Table 3). Mean HR and IQ correlated significantly negatively in all three coronary arteries. The correlation was strong for RCA reconstructed with CA and intermediate for MCA. Correlation was weak for LAD and LCx reconstructed with both CA and MCA. There was no significant correlation between IQ and BMI, age, ΔHR, or sex.

4 Discussion

In this study, we evaluated the performance of a novel deep learning-based MCA by comparing IQ of 64-MDCT-acquired CCTA images. As in previous studies, the RCA and its segments 1 and 2 were

found to be most prone to motion artifacts, as these are the most motile vessel segments [14]. MCA reconstruction had the greatest effect in these segments in improving IQ and reducing the total number of motion artifacts. Baseline IQ of LAD and LCx per artery and per segment was initially much better; MCA-improvement of LAD and LCx was negligible. On the per patient level, we observed an overall improvement of IQ. By evaluating potential disturbers, we found a significant negative correlation between mean HR and IQ for RCA, LAD, and LCx in CA- and MCA-reconstruction. However, the influence of mean HR was strong in the CA-reconstruction and intermediate in the MCA-reconstruction of the RCA. Correlation between mean HR and IQ of LAD and LCx was weak in both CA and MCA. BMI, age, sex, and ΔHR had no significant impact on IQ. The IQ results were correlated with mean HR, ΔHR, age, sex and BMI. Mean HR and BMI are already known to have a negative effect on IQ. Subsequently, we also correlated ΔHR to assess both its effect on IQ and the potential of the MCA used to mitigate this potential effect. We also

correlated age and sex to determine a possi-ble re-lated effect on IQ due to ageing effects or sex speci-ficities.

Recently, various MCA-based approaches have been published to mitigate motion artifacts. Two vendor-specific MCA are currently available: Snap-Shot Freeze (SSF) 1 and its successor SSF2 (GE Healthcare, Waukasha, WI, USA) [16,29]. In the clinical setting, SSF1 improved IQ and interpretability in ≥64-MDCT scanners independent of HR and BMI [36,39]. In addition, good IQ was maintained even at high HR, allowing wider application of PGI leading to a lower total effective dose [36,40]. Therefore, SSF1 is consid-ered a useful tool to assist CCTA in CCS diagnosis [49]. Positive effects of SSF2 on IQ are even more pro-found compared to its predecessor [16]. Unfortunately, both MCA are vendor-specific and only applicable on vendor-specific CT scanners [52]. Besides SSF1 and 2, there have been several attempts to develop even more effective and widely applicable MCA 11. How-ever, most of these suffer from limitations due to high effective dose, poor performance at high or irregular

HR, or long computation time [53,58,64,65]. The recently introduced deep-learning-based MCA might be a solution. Deep learning-based MCA can be applied post-acquisitionally without the need for raw data [66]. By this, they have a very short computation time and can be used vendor-independently [53,62]. However, larger studies on the performance of deep learning-based MCA are still scarce. Therefore, their clinical applicability cannot yet be assessed although phantom studies are promising [53,62,64].

In this study, we have found that the applied deep learning-based MCA *Deep PAMoCo* improves the IQ of 64-MDCT-acquired images [16,62]. By this, the rate of non-diagnostic images and false-positive results could be remarkably reduced, especially at higher HR [28,39,41]. As CCTA is already considered to have a high-negative predictive value, this could further increase its validity for the diagnosis of CCS [13]. Especially regarding its limited temporal resolution, the presented MCA seems to be attractive to enhance 64-MDCT-acquired images. However, the ap-

plied MCA can also be expected to be useful in combination with high-end imaging technology, as high or irregular HR can also disturb ≥128-MDCT and DSCT imaging [37]. Besides IQ improvement, the tested MCA could also reduce the effective dose during CCTA, as PGI could be applied at higher HR, and by this more widely [36,40]. However, as IQ still correlated with HR at an intermediate level, the presented MCA should be considered as a support and not as a substitute for HR control [42]. Finally, the tested MCA seems to be especially attractive in regard to its broad applicability due to its short computation time of 15 seconds per entire CCTA image and its vendor-independent use [52,53]. Thus, the presented MCA resembles a low-effort software upgrade for CCTA imaging performed with 64-MDCT.

This study has limitations. Firstly, since we wanted to test the ability of the MCA to compensate for motion artifacts and to improve IQ, patient data were not given in this trial. Secondly, in this study, we had to exclude eleven images completely and two

partially because of stack transition, vessel calcifications, and medical devices (stents and pacemakers) producing massive artifacts. In addition, due to a lack of documentation, we were unable to determine BMI in 20 patients and mean HR, ΔHR, age, and sex in 9 patients. Thirdly, the evaluation of IQ was conducted by a sole professional. Consequently, we cannot provide an inter-observer agreement. Fourthly, the IQ assessment was conducted by employing a five-point Likert score, consistent with previous research[51]. However, it is essential to note that there is no officially recommended approach for evaluating IQ, and therefore, the assessment lacks standardization. Consequently, the comparability with studies utilizing different assessment scores is restricted. Fifthly, the primary objective of this study was to evaluate the performance of the applied MCA in enhancing the IQ of real patient CCTA images. It is crucial to emphasize that the findings should not be generalized to other deep learning methods, given our limited study population and the focus on a sole MCA.

Sixthly, this was a single-center study. We recommend further studies at other radiology centers to increase the power and validity of our findings. Moreover, as this study aimed to evaluate the impact of a deep learning-based MCA on IQ, we cannot draw conclusions regarding its clinical utility. Further research is needed to evaluate the impact of MCA on diagnostic accuracy using invasive coronary angiography as a reference. Thus, it would also be possible to evaluate the impact of vessel calcification on IQ and MCA-related effective dose reduction. Finally, we did not compare the tested MCA with vendor-specific or other MCA. Thus, we cannot determine the superiority of the presented MCA.

5 Conclusion

In conclusion, this study has demonstrated on the one hand that the applied deep learning-based MCA is able to improve IQ in a large set of 64-MDCT acquired real-patient images and, on the other hand, to reduce HR impact on IQ. Thus, the presented MCA

can be considered as a promising example of deep learning-based MCA. Now, further comparative studies should be done to evaluate the effectiveness of the presented MCA in regard to other MCA and to assess its clinical utility and diagnostic accuracy.

6 Abbreviations

BMI= body mass index

CA = Conventional algorithm

CCTA = Coronary computed tomography angiography

CCS = Chronic coronary syndrome

DSCT = Dual source computed tomography

ECG = Electrocardiogram

ESC = European society of cardiology

FOV = Field of view

HR = Heart rate

IQ = Image quality

i.v. = intra-venously

LAD = Left descending artery

LCx = Left circumflex artery

MCA = Motion correction algorithm

MDCT = Multidetector computed tomography

PGI = Prospective electrocardiographic-gated imag-

ing

PTP = Pre-test probability
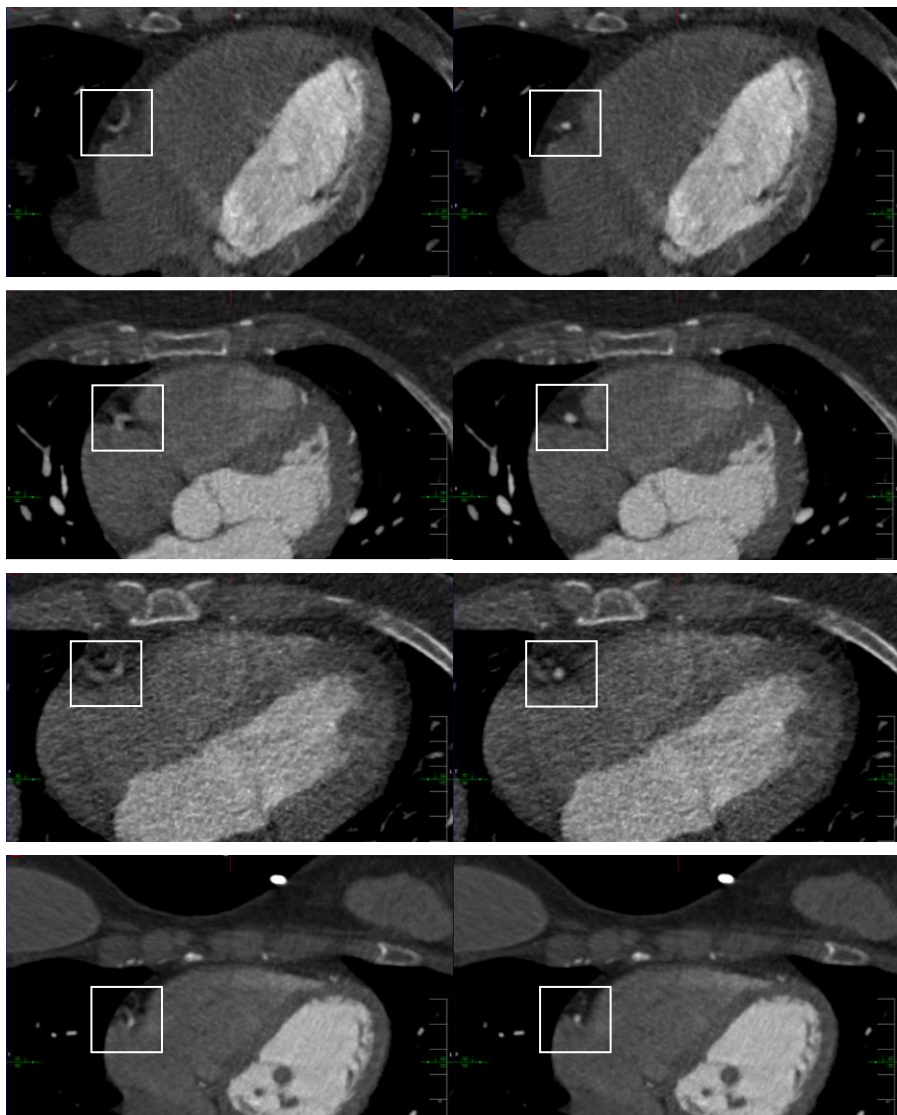
RBC = Rank-biserial correlation

RCA = Right coronary artery

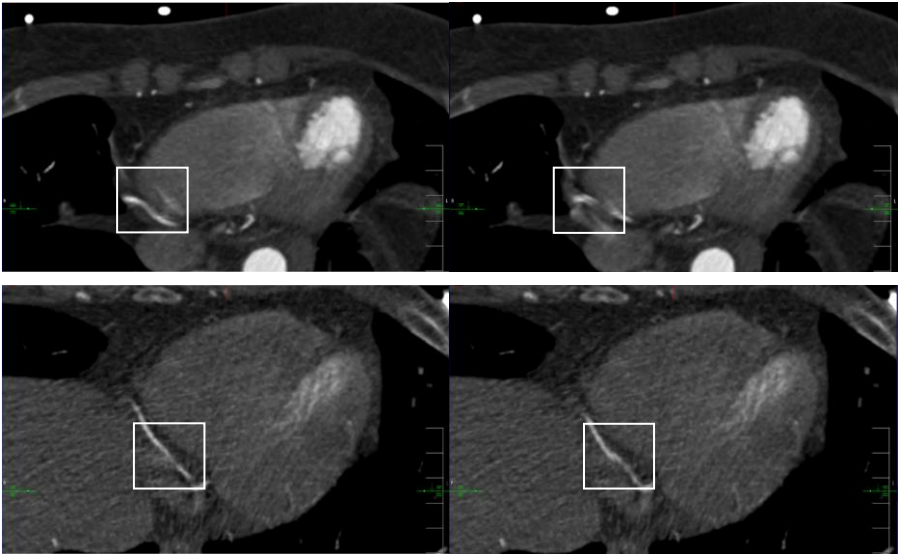SSF = SnapShot Freeze

ΔHR = intra-cycle HR changes

7 Supplementary Data

Motion artifact elimination by MCA

Supplementary Figure 1 Motion artifact elimination by MCA at segment 2

MCA inserted artifacts

*Supplementary Figure 3 MCA related artifacts (n=11)*

Image Quality

| Image Quality	1	2	3	4	5	1	2	3	4	5	p-value	Rank-biserial correlation
Per-Patient												
	2	9	26	48	29	2	3	21	42	46	**< .001**	-0.895
(%)	1,75	7,89	22,81	42,11	25,44	1,75	2,63	18,42	36,84	40,35		
Per-Artery												
RCA	11	29	35	19	16	7	13	25	37	28	**< .001**	-1.000
(%)	10,00	26,36	31,82	17,27	14,55	6,36	11,82	22,73	33,64	25,45		
LAD	2	2	10	33	66	2	2	11	28	70	0.175	-0.333
(%)	1,75	1,75	8,77	28,95	57,89	1,75	1,75	9,65	24,56	61,40		
LCx	3	8	18	24	57	3	7	21	21	58	0.558	0.028
(%)	2,70	7,21	16,22	21,62	51,35	2,70	6,31	18,92	18,92	52,25		
Per-Segment												
1	17	21	25	19	31	9	16	26	30	32	**< .001**	-0.674
(%)	15,04	18,58	22,12	16,81	27,43	7,96	14,16	23,01	26,55	28,32		
2	62	19	10	12	10	30	23	17	24	19	**< .001**	-1.000
(%)	54,87	16,81	8,85	10,62	8,85	26,55	20,35	15,04	21,24	16,81		
3	7	9	20	31	38	6	8	24	29	38	0.432	-0.043
(%)	6,67	8,57	19,05	29,52	36,19	5,71	7,62	22,86	27,62	36,19		
4	3	5	12	21	29	3	5	11	19	31	0.117	-0.600
(%)	4,29	7,14	17,14	30,00	41,43	4,35	7,25	15,94	27,54	44,93		
16	3	6	8	13	27	3	4	8	13	29	0.175	-0.333
(%)	5,26	10,53	14,04	22,81	47,37	5,26	7,02	14,04	22,81	50,88		
5	1	6	11	18	77	1	6	12	16	78	0.579	0.000
(%)	0,88	5,31	9,73	15,93	68,14	0,88	5,31	10,62	14,16	69,03		
6	1	5	26	14	67	1	5	24	14	69	0.036	-1.000
(%)	0,88	4,42	23,01	12,39	59,29	0,88	4,42	21,24	12,39	61,06		
7	0	12	24	13	64	0	12	25	10	66	0.383	-0.200
(%)	0,00	10,62	21,24	11,50	56,64	0,00	10,62	22,12	8,85	58,41		
8	0	18	21	16	58	0	16	22	14	61	**0.010**	-1.000
(%)	0,00	15,93	18,58	14,16	51,33	0,00	14,16	19,47	12,39	53,98		
9	9	19	19	8	49	9	18	18	7	51	0.036	-1.000
(%)	8,65	18,27	18,27	7,69	47,12	8,74	17,48	17,48	6,80	49,51		
10	9	28	12	8	44	9	26	11	7	48	**0.007**	-1.000
(%)	8,91	27,72	11,88	7,92	43,56	8,91	25,74	10,89	6,93	47,52		
11	4	17	26	10	54	4	17	26	10	53	0.500	-1.000
(%)	3,60	15,32	23,42	9,01	48,65	3,64	15,45	23,64	9,09	48,18		
12	15	9	11	7	31	15	9	11	5	33	0.173	-1.000
(%)	20,55	12,33	15,07	9,59	42,47	20,55	12,33	15,07	6,85	45,21		
13	5	19	18	17	44	5	17	20	17	44	0.286	-0.333
(%)	4,85	18,45	17,48	16,50	42,72	4,85	16,50	19,42	16,50	42,72		
14	15	11	9	2	31	15	11	9	1	32	0.500	-1.000
(%)	22,06	16,18	13,24	2,94	45,59	22,06	16,18	13,24	1,47	47,06		
15	0	0	4	1	3	0	0	4	1	3	0.500	-1.000
(%)	0,00	0,00	50,00	12,50	37,50	0,00	0,00	50,00	12,50	37,50		
17	1	8	3	5	15	1	6	4	4	16	0.173	-1.000

Supplementary Table 1 Image quality per-patient, per-artery, and per-segment due to a five-point Likert-scale, CA = conventional algorithm, MCA = motion correction algorithm, significant p-values in bold.

Correlation of Mean HR and Image Quality

A   LAD Image Quality and Mean HR
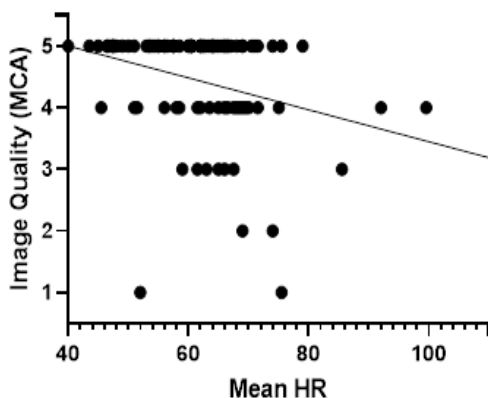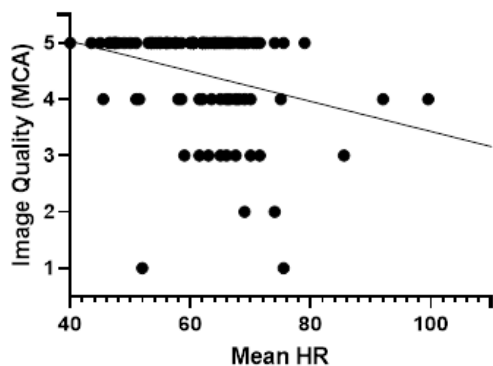
B   LCx Image Quality and Mean HR
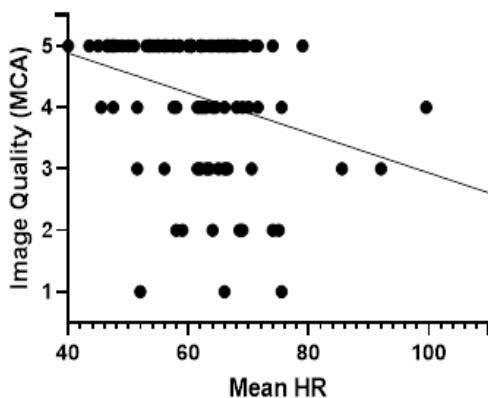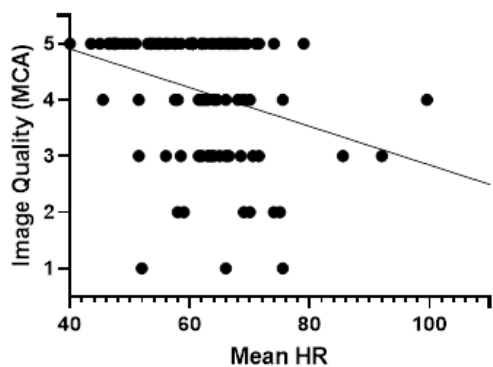
Supplementary Figure 3 (A) Correlation LAD and (B) LCx image quality and mean HR. 0.1=weak correlation, 0.3= moderate correlation, 0.5= strong correlation.

Impact of potentially disturbing factors

	CA			MCA		
	RCA	**LAD**	**LCx**	**RCA**	**LAD**	**LCx**
Gender						
Spearmans Rho	0.165	-0.003	-0.121	0.167	-0.061	-0.113
p-Wert	0.123	0.977	0.263	0.119	0.572	0.294
Age						
Spearmans Rho	2.366×10^{-4}	-0.063	0.032	0.016	-0.057	0.019
p-Wert	0.998	0.562	0.766	0.880	0.601	0.864
R-R						
Spearmans Rho	-0.117	-0.116	-0.078	-0.038	-0.121	-0.088
p-Wert	0.279	0.281	0.470	0.727	0.263	0.415
Mean HR						
Spearmans Rho	**-0.510**	**-0.295**	**-0.287**	**-0.403**	**-0.289**	**-0.328**
p-Wert	**< .001**	**0.005**	**0.007**	**< .001**	**0.006**	**0.002**
ΔHR						
Spearmans Rho	0.049	-0.110	-0.083	0.018	-0.155	-0.096
p-Wert	0.650	0.306	0.441	0.865	0.149	0.376
BMI						
	-0.095	-0.082	-0.062	0.022	-0.028	-0.046
	0.379	0.447	0.566	0.839	0.797	0.668

Supplementary Table 2 Correlation (Spearmans Rho and p-value) of Improvement per-artery and mean HR, ΔHR, BMI, age, and gender.

8 References

1. Miller JM, Rochitte CE, Dewey M, et al. Diagnostic performance of coronary angiography by 64-row CT. *N Engl J Med*. 2008;359(22):2324-2336. doi:10.1056/NEJMoa0806576

2. Mancini GBJ, Leipsic J, Budoff MJ, et al. CT Angiography Followed by Invasive Angiography in Patients With Moderate or Severe Ischemia-Insights From the ISCHEMIA Trial. *JACC Cardiovasc Imaging*. 2021;14(7):1384-1393. doi:10.1016/j.jcmg.2020.11.012

3. Maurovich-Horvat P, Bosserdt M, Kofoed KF, et al. CT or Invasive Coronary Angiography in Stable Chest Pain. *N Engl J Med*. 2022;386(17):1591-1602. doi:10.1056/NEJMoa2200963

4. Newby DE, Adamson PD, Berry C, et al. Coronary CT Angiography and 5-Year Risk of Myocardial Infarction. *N Engl J Med*. 2018;379(10):924-933. doi:10.1056/NEJMoa1805971

5. Bittner DO, Ferencik M, Douglas PS, Hoffmann U. Coronary CT Angiography as a Diagnostic and Prognostic Tool: Perspective from a Multicenter

Randomized Controlled Trial: PROMISE. *Curr Cardiol Rep*. 2016;18(5):40. doi:10.1007/s11886-016-0718-9

6. Arora N, Matheny ME, Sepke C, Resnic FS. A propensity analysis of the risk of vascular complications after cardiac catheterization procedures with the use of vascular closure devices. *Am Heart J*. 2007;153(4):606-611.
doi:10.1016/j.ahj.2006.12.014

7. Noto TJ, Johnson LW, Krone R, et al. Cardiac catheterization 1990: a report of the Registry of the Society for Cardiac Angiography and Interventions (SCA&I). *Cathet Cardiovasc Diagn*. 1991;24(2):75-83. doi:10.1002/ccd.1810240202

8. Balaney B, Vembar M, Grass M, et al. Improved visualization of the coronary arteries using motion correction during vasodilator stress CT myocardial perfusion imaging. *Eur J Radiol*. 2019;114:1-5. doi:10.1016/j.ejrad.2019.02.010.

9. Soschynski M, Taron J, Schlett CL, Bamberg F, Krauß T. Update Kardio-CT – mehr als nur anato-

mische Bildgebung? : Aktuelle Leitlinien und funk-
tionelle CT-Techniken zur Stenosequantifizie-
rung. *Radiologe*. 2020;60(12):1131-1141.
doi:10.1007/s00117-020-00767-2

10. Montalescot G, Sechtem U, Achenbach S, et al.
2013 ESC guidelines on the management of sta-
ble coronary artery disease: the Task Force on the
management of stable coronary artery disease of
the European Society of Cardiology. *Eur Heart J*.
2013;34(38):2949-3003.
doi:10.1093/eurheartj/eht296

11. Foldyna B, Udelson JE, Karády J, et al. Pretest
probability for patients with suspected obstructive
coronary artery disease: re-evaluating Diamond–
Forrester for the contemporary era and clinical im-
plications: insights from the PROMISE trial. *Eur
Heart J Cardiovasc Imaging*. 2018;20(5):574-581.
doi:10.1093/ehjci/jey182

12. Feger S, Ibes P, Napp AE, et al. Clinical pre-test
probability for obstructive coronary artery dis-
ease: insights from the European DISCHARGE

pilot study. *Eur Radiol*. 2021;31(3):1471-1481. doi:10.1007/s00330-020-07175-z

13. Knuuti J, Wijns W, Saraste A, et al. 2019 ESC Guidelines for the diagnosis and management of chronic coronary syndromes. *Eur Heart J*. 2020;41(3):407-477.
    doi:10.1093/eurheartj/ehz425

14. Husmann L, Leschka S, Desbiolles L, et al. Coronary artery motion and cardiac phases: dependency on heart rate -- implications for CT image reconstruction. *Radiology*. 2007;245(2):567-576. doi:10.1148/radiol.2451061791

15. Aghayev A, Murphy DJ, Keraliya AR, Steigner ML. Recent developments in the use of computed tomography scanners in coronary artery imaging. *Expert Rev Med Devices*. 2016;13(6):545-553. doi:10.1080/17434440.2016.1184968

16. Liang J, Sun Y, Ye Z, et al. Second-generation motion correction algorithm improves diagnostic accuracy of single-beat coronary CT angiography in patients with increased heart rate. *Eur Radiol*.

2019;29(8):4215-4227. doi:10.1007/s00330-018-5929-6

17. Rybicki FJ, Otero HJ, Steigner ML, et al. Initial evaluation of coronary images from 320-detector row computed tomography. *Int J Cardiovasc Imaging*. 2008;24(5):535-546. doi:10.1007/s10554-008-9308-2

18. Achenbach S, Ropers U, Kuettner A, et al. Randomized comparison of 64-slice single- and dual-source computed tomography coronary angiography for the detection of coronary artery disease. *JACC Cardiovasc Imaging*. 2008;1(2):177-186. doi:10.1016/j.jcmg.2007.11.006

19. Achenbach S, Marwan M, Schepis T, et al. High-pitch spiral acquisition: a new scan mode for coronary CT angiography. *J Cardiovasc Comput Tomogr*. 2009;3(2):117-121. doi:10.1016/j.jcct.2009.02.008

20. Sun Z, Choo GH, Ng KH. Coronary CT angiography: current status and continuing challenges. *Br J Radiol*. 2012;85(1013):495-510. doi:10.1259/bjr/15296170

21. Horiguchi J, Nakanishi T, Tamura A, Ito K, Sasaki K, Shen Y. Technical innovation of cardiac multi-row detector CT using multisector reconstruction. *Comput Med Imaging Graph*. 2002;26(4):217-226. doi:10.1016/s0895-6111(02)00010-1

22. Machida H, Tanaka I, Fukui R, et al. Current and Novel Imaging Techniques in Coronary CT. *Radiographics*. 2015;35(4):991-1010. doi:10.1148/rg.2015140181

23. Sabarudin A, Sun Z, Yusof AKM. Coronary CT angiography with single-source and dual-source CT: comparison of image quality and radiation dose between prospective ECG-triggered and retrospective ECG-gated protocols. *Int J Cardiol*. 2013;168(2):746-753. doi:10.1016/j.ijcard.2012.09.217

24. Maurer MH, Hamm B, Dewey M. Survey regarding the clinical practice of cardiac CT in Germany: indications, scanning technique and reporting. *Rofo*. 2009;181(12):1135-1143. doi:10.1055/s-0028-1109621

25. Kutaiba N, Lukies M, Galea M, et al. The effects of sublingual nitroglycerin administration in coronary computed tomography angiography. *Clin Imaging*. 2020;60(2):194-199. doi:10.1016/j.clinimag.2019.11.019

26. Shapiro MD, Pena AJ, Nichols JH, et al. Efficacy of pre-scan beta-blockade and impact of heart rate on image quality in patients undergoing coronary multidetector computed tomography angiography. *Eur J Radiol*. 2008;66(1):37-41. doi:10.1016/j.ejrad.2007.05.006

27. Graaf FR de, Schuijf JD, van Velzen JE, et al. Evaluation of contraindications and efficacy of oral Beta blockade before computed tomographic coronary angiography. *Am J Cardiol*. 2010;105(6):767-772. doi:10.1016/j.amjcard.2009.10.058

28. Sun J, Okerlund D, Cao Y, et al. Further Improving Image Quality of Cardiovascular Computed Tomography Angiography for Children With High Heart Rates Using Second-Generation Motion Correction Algorithm. *J Comput Assist Tomogr*.

2020;44(5):790-795.
doi:10.1097/RCT.0000000000001035

29. Leipsic J, Labounty TM, Hague CJ, et al. Effect of a novel vendor-specific motion-correction algorithm on image quality and diagnostic accuracy in persons undergoing coronary CT angiography without rate-control medications. *J Cardiovasc Comput Tomogr*. 2012;6(3):164-171. doi:10.1016/j.jcct.2012.04.004

30. Park JB, Jeong YJ, Lee G, Lee NK, Kim JY, Lee JW. Influence of Heart Rate and Innovative Motion-Correction Algorithm on Coronary Artery Image Quality and Measurement Accuracy Using 256-Detector Row Computed Tomography Scanner: Phantom Study. *Korean J Radiol*. 2019;20(1):94-101. doi:10.3348/kjr.2018.0251

31. Xing Y, Zhao Y, Guo N, et al. Effect of a Novel Intracycle Motion Correction Algorithm on Dual-Energy Spectral Coronary CT Angiography: A Study with Pulsating Coronary Artery Phantom at High Heart Rates. *Korean J Radiol*. 2017;18(6):881-887. doi:10.3348/kjr.2017.18.6.881

32. Cho I, Elmore K, Ó Hartaigh B, et al. Heart-rate dependent improvement in image quality and diagnostic accuracy of coronary computed tomographic angiography by novel intracycle motion correction algorithm. *Clin Imaging*. 2015;39(3):421-426. doi:10.1016/j.clinimag.2014.11.020.

33. Chen Z, Contijoch F, Schluchter A, et al. Precise measurement of coronary stenosis diameter with CCTA using CT number calibration. *Med Phys*. 2019;46(12):5514-5527. doi:10.1002/mp.13862

34. Liang J, Wang H, Xu L, et al. Diagnostic performance of 256-row detector coronary CT angiography in patients with high heart rates within a single cardiac cycle: a preliminary study. *Clin Radiol*. 2017;72(8):694.e7-694.e14. doi:10.1016/j.crad.2017.03.004

35. Pontone G, Andreini D, Bertella E, et al. Impact of an intra-cycle motion correction algorithm on overall evaluability and diagnostic accuracy of computed tomography coronary angiography. *Eur*

Radiol. 2016;26(1):147-156. doi:10.1007/s00330-015-3793-1

36. Machida H, Lin X-Z, Fukui R, et al. Influence of the motion correction algorithm on the quality and interpretability of images of single-source 64-detector coronary CT angiography among patients grouped by heart rate. *Jpn J Radiol*. 2015;33(2):84-93. doi:10.1007/s11604-014-0382-1

37. Liang J, Wang H, Xu L, et al. Impact of SSF on Diagnostic Performance of Coronary Computed Tomography Angiography Within 1 Heart Beat in Patients With High Heart Rate Using a 256-Row Detector Computed Tomography. *J Comput Assist Tomogr*. 2018;42(1):54-61. doi:10.1097/RCT.0000000000000641

38. Wen B, Xu L, Liang J, Fan Z, Sun Z. A Preliminary Study of Computed Tomography Coronary Angiography Within a Single Cardiac Cycle in Patients With Atrial Fibrillation Using 256-Row Detector Computed Tomography. *J Comput Assist Tomogr*.

2018;42(2):277-281.

doi:10.1097/RCT.0000000000000683

39. Fuchs TA, Stehli J, Dougoud S, et al. Impact of a new motion-correction algorithm on image quality of low-dose coronary CT angiography in patients with insufficient heart rate control. *Acad Radiol*. 2014;21(3):312-317.

doi:10.1016/j.acra.2013.10.014

40. Li Z-N, Yin W-H, Lu B, et al. Improvement of Image Quality and Diagnostic Performance by an Innovative Motion-Correction Algorithm for Prospectively ECG Triggered Coronary CT Angiography. *PLoS One*. 2015;10(11):e0142796.

doi:10.1371/journal.pone.0142796

41. Andreini D, Pontone G, Mushtaq S, et al. Low-dose CT coronary angiography with a novel Intra-Cycle motion-correction algorithm in patients with high heart rate or heart rate variability. *Eur Heart J Cardiovasc Imaging*. 2015;16(10):1093-1100.

doi:10.1093/ehjci/jev033

42. Sheta HM, Egstrup K, Husic M, Heinsen LJ, Nieman K, Lambrechtsen J. Impact of a motion correction algorithm on image quality in patients undergoing CT angiography: A randomized controlled trial. *Clin Imaging*. 2017;42:1-6. doi:10.1016/j.clinimag.2016.11.002

43. Modica MJ, Kanal KM, Gunn ML. The obese emergency patient: imaging challenges and solutions. *Radiographics*. 2011;31(3):811-823. doi:10.1148/rg.313105138

44. Latif MA, Sanchez FW, Sayegh K, et al. Volumetric Single-Beat Coronary Computed Tomography Angiography: Relationship of Image Quality, Heart Rate, and Body Mass Index. Initial Patient Experience With a New Computed Tomography Scanner. *J Comput Assist Tomogr*. 2016;40(5):763-772. doi:10.1097/RCT.0000000000000428

45. Andreini D, Pontone G, Mushtaq S, et al. Diagnostic accuracy of coronary CT angiography performed in 100 consecutive patients with coronary stents using a whole-organ high-definition CT

scanner. *Int J Cardiol*. 2019;274:382-387. doi:10.1016/j.ijcard.2018.09.010

46. Shah NR, Blankstein R, Villines T, Imran H, Morrison AR, Cheezum MK. Coronary CTA for Surveillance of Cardiac Allograft Vasculopathy. *Curr Cardiovasc Imaging Rep*. 2018;11(11):26. doi:10.1007/s12410-018-9467-z

47. Andreini D, Lin FY, Rizvi A, et al. Diagnostic Performance of a Novel Coronary CT Angiography Algorithm: Prospective Multicenter Validation of an Intracycle CT Motion Correction Algorithm for Diagnostic Accuracy. *AJR Am J Roentgenol*. 2018;210(6):1208-1215. doi:10.2214/AJR.17.18670

48. Sheta HM, Egstrup K, Husic M, Heinsen LJ, Lambrechtsen J. Impact of a motion correction algorithm on quality and diagnostic utility in unselected patients undergoing coronary CT angiography. *Clin Imaging*. 2016;40(2):217-221. doi:10.1016/j.clinimag.2015.10.007

49. Lee H, Kim JA, Lee JS, Suh J, Paik SH, Park JS. Impact of a vendor-specific motion-correction algorithm on image quality, interpretability, and diagnostic performance of daily routine coronary CT angiography: influence of heart rate on the effect of motion-correction. *Int J Cardiovasc Imaging*. 2014;30(8):1603-1612. doi:10.1007/s10554-014-0499-4

50. Machida H, Fukui R, Gao J, et al. Reduction of Coronary Motion Artifacts in Prospectively Electrocardiography-Gated Coronary Computed Tomography Angiography Using Monochromatic Imaging at Various Energy Levels in Combination With a Motion Correction Algorithm on Single-Source Fast Tube Voltage Switching Dual-Energy Computed Tomography: A Phantom Experiment. *Invest Radiol*. 2016;51(8):513-519. doi:10.1097/RLI.0000000000000263

51. Carrascosa P, Deviggiano A, Leipsic JA, et al. Dual energy imaging and intracycle motion correction for CT coronary angiography in patients

with intermediate to high likelihood of coronary artery disease. *Clin Imaging*. 2015;39(6):1000-1005. doi:10.1016/j.clinimag.2015.07.023

52. Ren P, He Y, Zhu Y, et al. Motion artefact reduction in coronary CT angiography images with a deep learning method. *BMC Med Imaging*. 2022;22(1):184. doi:10.1186/s12880-022-00914-2

53. Lossau Née Elss T, Nickisch H, Wissel T, et al. Motion estimation and correction in cardiac CT angiography images using convolutional neural networks. *Comput Med Imaging Graph*. 2019;76:101640. doi:10.1016/j.compmedimag.2019.06.001

54. van Stevendaal U, Berg J von, Lorenz C, Grass M. A motion-compensated scheme for helical cone-beam reconstruction in cardiac CT angiography. *Med Phys*. 2008;35(7):3239-3251. doi:10.1118/1.2938733

55. Schwemmer C, Rohkohl C, Lauritsch G, Müller K, Hornegger J. Residual motion compensation in

ECG-gated interventional cardiac vasculature re-construction. *Phys Med Biol*. 2013;58(11):3717-3737. doi:10.1088/0031-9155/58/11/3717

56. Muller K, Rohkohl C, Lauritsch G, et al. 4-D motion field estimation by Combined Multiple Heart Phase Registration (CMHPR) for cardiac C-arm data. In: 2012 IEEE Nuclear Science Symposium and Medical Imaging Conference Record (NSS/MIC). IEEE; 2012:3707-3712.

57. Bhagalia R, Pack JD, Miller JV, Iatrou M. Nonrigid registration-based coronary artery motion correction for cardiac computed tomography. *Med Phys*. 2012;39(7):4245-4254. doi:10.1118/1.4725712

58. Rohkohl C, Bruder H, Stierstorfer K, Flohr T. Improving best-phase image quality in cardiac CT by motion correction with MAM optimization. *Med Phys*. 2013;40(3):31901. doi:10.1118/1.4789486

59. Pack, Edic, Claus, Iatrou, and Miller., inventor. Method for computed tomography motion estimation and compensation. US8,224,056.

60. Kim S, Chang Y, Ra JB. Cardiac motion correction based on partial angle reconstructed images in x-

ray CT. *Med Phys*. 2015;42(5):2560-2571. doi:10.1118/1.4918580

61. Hahn J, Bruder H, Allmendinger T, Stierstorfer K, Flohr T, Kachelriess M. Reduction of motion artifacts in cardiac CT based on partial angle reconstructions from short scan data. In: Kontos D, Flohr TG, Lo JY, eds. Medical Imaging 2016: Physics of Medical Imaging. SPIE; 2016:97831A.

62. Maier J, Lebedev S, Erath J, et al. Deep learning-based coronary artery motion estimation and compensation for short-scan cardiac CT. *Med Phys*. 2021;48(7):3559-3571. doi:10.1002/mp.14927

63. Principe JC. *Information Theoretic Learning: Renyi's Entropy and Kernel Perspectives*. Springer New York; Imprint: Springer; 2010.

64. Kim S, Chang Y, Ra JB. Cardiac Motion Correction for Helical CT Scan With an Ordinary Pitch. *IEEE Trans Med Imaging*. 2018;37(7):1587-1596. doi:10.1109/TMI.2018.2817594

65. Hahn J, Bruder H, Rohkohl C, et al. Motion compensation in the region of the coronary arteries

based on partial angle reconstructions from short-scan CT data. *Med Phys*. 2017;44(11):5795-5813. doi:10.1002/mp.12514

66. *2016 IEEE Conference on Computer Vision and Pattern Recognition (CVPR)*. IEEE; 2016.

67. Goodfellow IJ, Pouget-Abadie J, Mirza M, et al. *Generative Adversarial Networks*; 2014. https://arxiv.org/pdf/1406.2661.

68. Jung S, Lee S, Jeon B, Jang Y, Chang H-J. Deep Learning Cross-Phase Style Transfer for Motion Artifact Correction in Coronary Computed Tomography Angiography. *IEEE Access*. 2020;8:81849-81863. doi:10.1109/ACCESS.2020.2991445

69. Deng F, Tie C, Zeng Y, et al. Correcting motion artifacts in coronary computed tomography angiography images using a dual-zone cycle generative adversarial network. *J Xray Sci Technol*. 2021;29(4):577-595. doi:10.3233/XST-210841

70. Lossau T, Nickisch H, Wissel T, et al. Motion artifact recognition and quantification in coronary CT angiography using convolutional neural networks.

Med Image Anal. 2019;52:68-79. doi:10.1016/j.media.2018.11.003

71. Narula J, Chandrashekhar Y, Ahmadi A, et al. SCCT 2021 Expert Consensus Document on Coronary Computed Tomographic Angiography: A Report of the Society of Cardiovascular Computed Tomography. *J Cardiovasc Comput Tomogr*. 2021;15(3):192-217. doi:10.1016/j.jcct.2020.11.001.

72. Leipsic J, Abbara S, Achenbach S, et al. SCCT guidelines for the interpretation and reporting of coronary CT angiography: a report of the Society of Cardiovascular Computed Tomography Guidelines Committee. *J Cardiovasc Comput Tomogr*. 2014;8(5):342-358. doi:10.1016/j.jcct.2014.07.003

9 Acknowledgements

Optimizing Coronary Computed Tomography Angiography Using a Novel Deep Learning-Based Algorithm

H. J. H. Dreesen[1,2] · C. Stroszczynski[1] · M. M. Lell[2]

Abstract

Coronary computed tomography angiography (CCTA) is an essential part of the diagnosis of chronic coronary syndrome (CCS) in patients with low-to-intermediate pre-test probability. The minimum technical requirement is 64-row multidetector CT (64-MDCT), which is still frequently used, although it is prone to motion artifacts because of its limited temporal resolution and z-coverage. In this study, we evaluate the potential of a deep-learning-based motion correction algorithm (MCA) to eliminate these motion artifacts. 124 64-MDCT-acquired CCTA examinations with at least minor motion artifacts were included. Images were reconstructed using a conventional reconstruction algorithm (CA) and a MCA. Image quality (IQ), according to a 5-point Likert score, was evaluated per-segment, per-artery, and per-patient and was correlated with potentially disturbing factors (heart rate (HR), intra-cycle HR changes, BMI, age, and sex). Comparison was done by Wilcoxon-Signed-Rank test, and correlation by Spearman's Rho. Per-patient, insufficient IQ decreased by 5.26%, and sufficient IQ increased by 9.66% with MCA. Per-artery, insufficient IQ of the right coronary artery (RCA) decreased by 18.18%, and sufficient IQ increased by 27.27%. Per-segment, insufficient IQ in segments 1 and 2 decreased by 11.51% and 24.78%, respectively, and sufficient IQ increased by 10.62% and 18.58%, respectively. Total artifacts per-artery decreased in the RCA from 3.11 ± 1.65 to 2.26 ± 1.52. HR dependence of RCA IQ decreased to intermediate correlation in images with MCA reconstruction. The applied MCA improves the IQ of 64-MDCT-acquired images and reduces the influence of HR on IQ, increasing 64-MDCT validity in the diagnosis of CCS.

Keywords Coronary computed tomography angiography · Single-source computed tomography · 64-Detector row computed tomography · Motion artifact reduction · Deep learning-based algorithm · Motion correction algorithm

Introduction

The European Society of Cardiology (ESC) recommends coronary computed tomography angiography (CCTA) as the diagnostic method of choice for patients with suspected chronic coronary syndrome (CCS) with a low to intermediate pre-test probability (PTP) [1]. Currently, 64-row multidetector single-source CT (64-MDCT) is considered the minimum requirement for proper CCTA imaging [2]. The 64-MDCT systems have been shown to be a valid and accurate diagnostic tool, even when compared to ≥ 128-MDCT or dual-source CT (DSCT) [3, 4]. In addition, 64-MDCT is widely available, making it an indispensable diagnostic tool in patients with CCS [1, 5, 6]. Although 64-MDCT can provide perfect images under optimal conditions, its limited temporal resolution makes it susceptible to motion artifacts in patients with high or variable heart rates (HR), especially in the right coronary artery (RCA) [1, 7, 8]. Several approaches have been proposed to reduce motion artifacts in 64-MDCT, both in terms of hardware modification (gantry rotation time, half scan rotation, high-pitch imaging, prospective (PGI) and retrospective electrocardiographic (ECG)-gated imaging) and HR control (beta-blockers or ivabradine) [3, 4, 8, 9]. However, these approaches have limitations either due to physical limits or contraindications [9, 10]. For further image enhancement, novel software-based approaches in the form of motion correction algorithms (MCA) offer a suitable solution for motion-disturbed images.

✉ H. J. H. Dreesen
Hendrik.dreesen@web.de

1 Department of Radiology, University Regensburg, Franz-Josef-Strauss Allee 11, 93053 Regensburg, Germany

2 Department of Radiology, Neuroradiology and Nuclear Medicine, Klinikum Nürnberg, Paracelsus Medical University, Nuremberg, Germany

Several MCA based on different technical approaches have been introduced in the last decade [11]. However, only a few MCA have proven their clinical utility and are commercially available [12, 13]. Furthermore, the clinical applicability of most of these MCA is limited mainly because of either vendor-specificity, high effective dose, poor performance at high or irregular HR, or long computation time [11, 14–16]. The latest MCA variants are based on deep-learning networks [11]. In several phantom trials and small patient studies, they have shown remarkable results in improving the image quality (IQ) of motion-impaired images in an acceptable computation time [11, 14, 17]. However, clinical data for these deep learning-based MCA are still scarce. The aim of this study was to evaluate the performance of a recently introduced deep learning-based MCA (*Deep PAMoCo*) on IQ in a large set of real-world patient CCTA data sets and to demonstrate the potential clinical utility of this MCA [15].

Materials and Methods

Image Data, Algorithm, and CT-Scanning

124 CCTA data sets of consecutive patients scanned with the same 64-MDCT system and the same CT protocol were retrieved from the Picture Archiving and Communication System and included in this study. The clinical indication for CCTA was according to clinical guidelines [2]. Original image data were anonymized, and patients are not identifiable. Consecutive patient data in which at least one vascular segment was affected by motion artifacts were selected for the evaluation with a conventional reconstruction algorithm (CA) and the MCA. Since the MCA is applied to already reconstructed image data, no raw data is required. The MCA can, therefore, be used on different CT systems without any limitations.

The function of the applied MCA is based on partial angle reconstructions (PAR) computed with a motion vector field (MVF) generated by a Deep Neural Network (DNN). After an initial reconstruction of the CCTA images, the position of the coronary arteries is determined using a segmentation software. PAR of the coronary arteries are created from this data by forward and backprojecting data. PAR are characterized by a very high temporal resolution, virtually freezing the individual PAR. The PAR are then mapped by a MVF to the same motion state. MVF are generated by a DNN and compute a motion vector for each PAR. Finally, the motion-corrected PAR are re-inserted into the original reconstruction, resulting in a motion-compensated image. More detailed technical information about the MCA can be found elsewhere [15].

The scanning protocol included calcium-scoring, test-bolus-tracking, and CCTA. CCTA imaging was performed using a 64-MDCT (Siemens Definition 64,

Siemens Healthineers, Erlangen, Germany) with a gantry rotation time of 0.33s, a collimation of 64×0.6mm, an automatic, weight-adjusted tube voltage between 100 and 120kVp, and automatic exposure control. Acquisition was performed with PGI. PGI was performed at a maximum HR ≤ 80 beats per minute (bpm) during an R-R interval of 60–80% in diastole (average 68%). Low-dose calcium-scoring was performed before CCTA to estimate the patient's calcium load. A calcium score of 1000 was considered the upper limit for CCTA. Patients with a calcium score >1000 were referred to the catheter laboratory. CCTA was performed by trained staff. Beta-blockers were administered orally or i.v. if HR was ≥ 65bpm after checking contraindications. Sublingual nitroglycerine was administered 2–3min before the examination. For the examination, patients were placed in the supine position, head first. The field of view (FOV) was estimated considering the size of the heart (approximately from 2cm below the carina to the lower edge of the apex cordis). Contrast medium (CM; Solutrast 370, Bracco, Milan, Italy) was administered via an antecubital intravenous line at a flow rate of 6ml/s followed by 30ml of saline at the same flow rate. Body mass index (BMI), age, sex, mean HR, and intra-cycle HR changes (ΔHR) were registered.
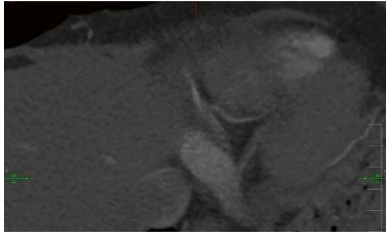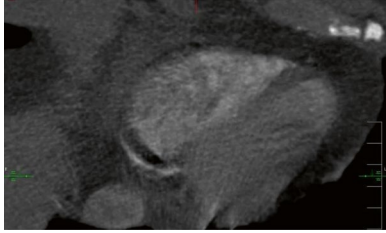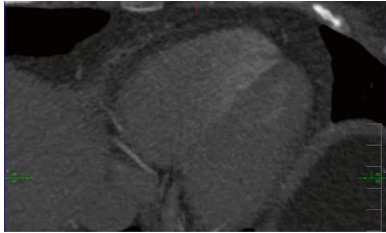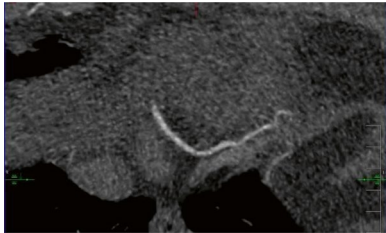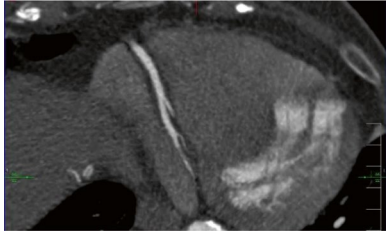
Image Quality Assessment

Images were evaluated by a radiology resident trained for the evaluation of CCTA images. IQ was assessed per-segment, per-artery (right coronary artery=RCA, left anterior descending artery=LAD, left circumflex artery=LCx), and per-patient. Per-segment assessment was performed in regard to the Society of Cardiovascular Computed Tomography-guidelines for the interpretation and reporting of CCTA [18] using a 17-segment approach. A minimal vessel diameter of 2mm was chosen for quality evaluation. IQ was determined using a 5-point Likert score in terms of image evaluability. The 5-point Likert score provides accurate information on IQ without being overwhelming. Evaluability was determined based on image readability and the amount of motion artifacts according to previous studies [19]: 1=unacceptable; 2=below average; 3=average; 4=above average; 5=excellent (Table 1). The total amount of motion artifacts was assessed by counting the motion artifacts per-artery (RCA, LAD, LCx) by identifying typical patterns of motion artifacts as "crescents," "tails," and "horns" (Fig. 1A). MCA-inserted artifacts were assessed by identifying typical patterns as "steps" or vessel "duplications" (Fig. 1B).

Statistics

Statistical analysis was carried out with JASP team (2022). JASP (version 0.16.4) [computer software].

**Table 1** Likert score description

Likert Score description

Likert score 1	Unacceptable: image is not diagnostic due to massive motion artifacts	
Likert score 2	Below average: image is suboptimal and not diagnostic due to severe motion artifacts	
Likert score 3	Average: image is readable and diagnostic, slight to moderate motion artifacts are apparent	
Likert score 4	Above average: image has good IQ; slight motion artifacts are apparent	
Likert score 5	Excellent: image is perfectly readable; no artifacts are apparent	

Continuous variables are expressed as mean $\pm$ standard deviation (SD). The central tendency of non-dichotomous categorical variables is expressed as median and percentage. Significance was tested using paired samples tests. A one-tailed p-value of <0.01 is considered to indicate statistical significance in IQ assessment. IQ between the CA and the MCA was compared using the Wilcoxon-Signed-Rank test for ordinal variables. Rank-Biserial correlation was chosen as the effect size measurement. Normality of continuous data was assessed by applying the Shapiro–Wilk test. As continuous data were not normally distributed, the non-parametric

Fig. 1 **A** Motion artifact elimination by MCA at segment 2. **B** MCA inserted artifacts at segment 3 ($n = 11$)

Illustration of MCA function
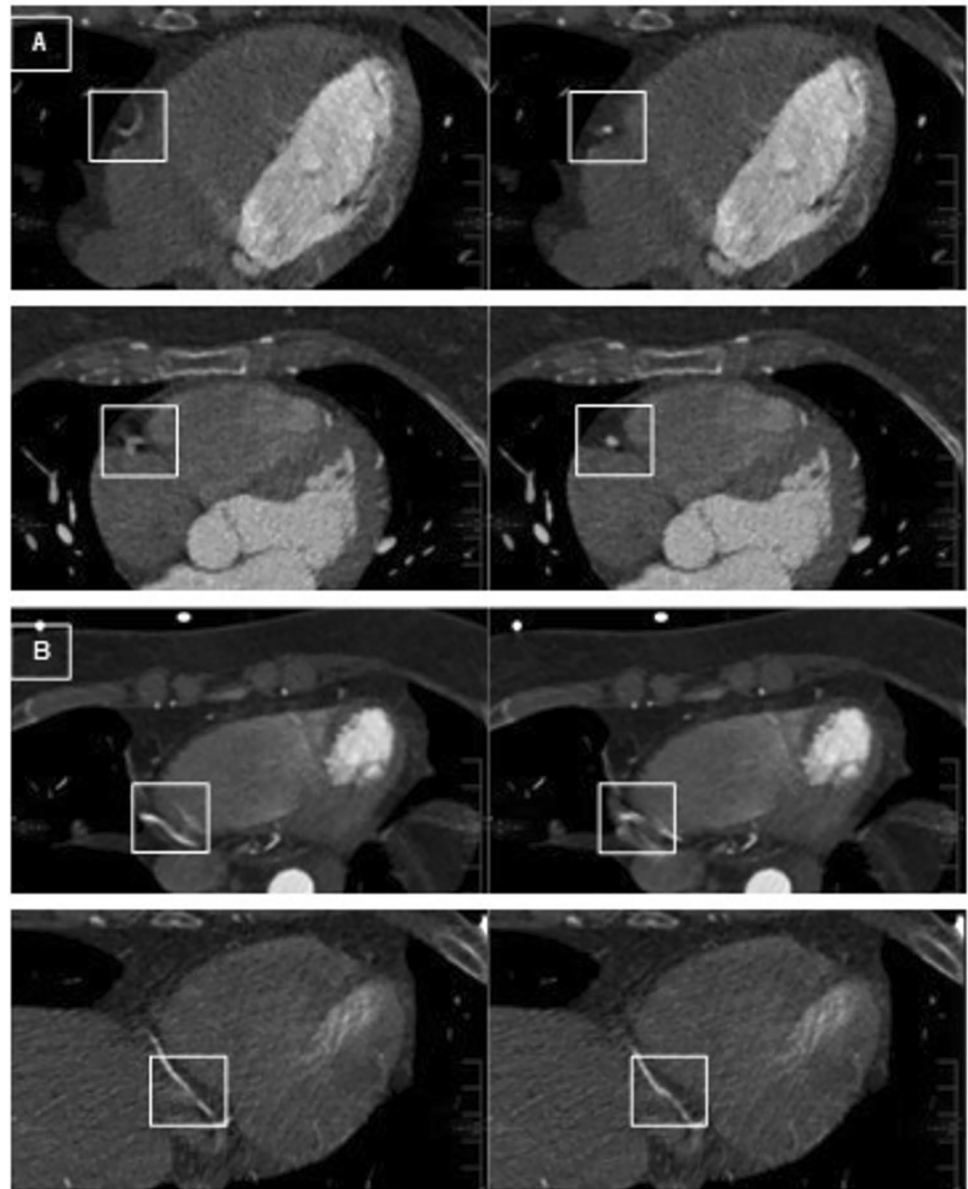
Wilcoxon-Signed-Rank test and Rank-Biserial correlation were applied. Correlation analysis between BMI, age, sex, mean HR, and ΔHR and IQ was performed using Spearman's Rho. A two-tailed *p*-value of <0.01 is considered to indicate statistical significance. Graphs were created using GraphPad Prism, Prism 9 for Windows 64-bit, version 9.5.1 (733), January 26, 2023, tables were created using Microsoft® Excel® 2019 MSO (Version 2303 Build 16.0.16227.20202) 64 Bit.

Results

CCTA data sets of 124 patients were evaluated (Table 2). Of these, eleven data sets were excluded due to severe stack transition, vessel calcifications, and medical devices (stents and pacemakers) producing massive artifacts. BMI was missing in 20 patients; sex, age, ΔHR, and mean HR in nine patients. IQ of 113 patients, 333 arteries, and 3019 segments was evaluated (Fig. 2 and 3; Supplementary Table 1).

Table 2 Study population

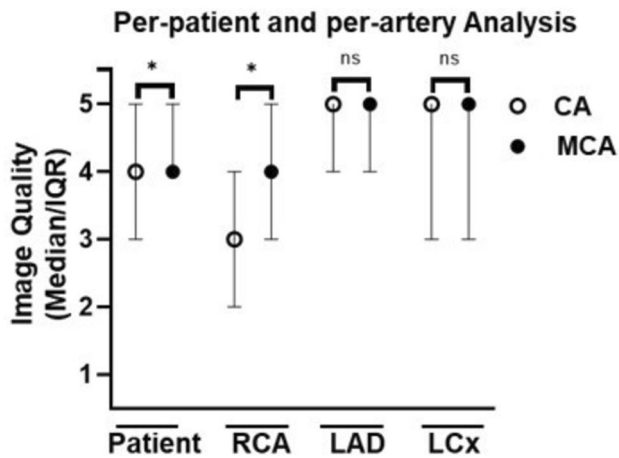| Study population			
Total (*n*)	124		
Male/female	59	55	
	Mean	Range	$\pm$ SD
Mean age (years)	59,49	21–95	12,53
Mean BMI (kg/m^2)	27,58	18,9–43,03	5,21
Mean HR (bpm)	63,92	43–133	11,88
Mean ΔHR (bpm)	7,14	0–105	14,16

Fig. 2 Median and interquartile range of IQ per-patient and per-artery with CA and MCA due to a 5-point Likert score. Significance is marked with an asterisk

Per-patient, unacceptable or below-average images decreased from 9.65% to 4.39%, and above-average or excellent images increased from 67.54% to 77.2%. Per-artery, the RCA improved significantly. Here, the percentage of unacceptable or below-average images decreased from 36.36% to 18.18%, and above-average or excellent images increased from 31.82% to 59.09%. Per-segment, RCA segments 1 and 2 benefited from the MCA. Unacceptable or below-average images decreased from 33.63% to 22.12% and from 71.68% to 46.9%, respectively, while above-average or excellent images increased from 44.25% to 54.87% and from 19.47% to 38.05%, respectively. The total number of artifacts was determined per-artery (Fig. 4; Supplementary Table 2). We observed a decrease in motion artifacts from 3.11 ± 1.65 to 2.26 ± 1.52 in the RCA. There was no significant decrease in motion artifacts in the LAD or LCx. In 11 out of 3019 segments, the IQ deteriorated due to MCA-inserted artifacts, especially in RCA segments 1 and 3. These artifacts mostly resembled vessel "duplications" or "steps". The correlation between IQ and BMI, age, mean HR, ΔHR, and sex was tested per-artery using Spearman's Rho (Fig. 5; Supplementary Table 3). Mean HR and IQ correlated significantly negatively in all three coronary arteries. The correlation was strong for RCA reconstructed with CA and intermediate for MCA. Correlation was weak for LAD and LCx
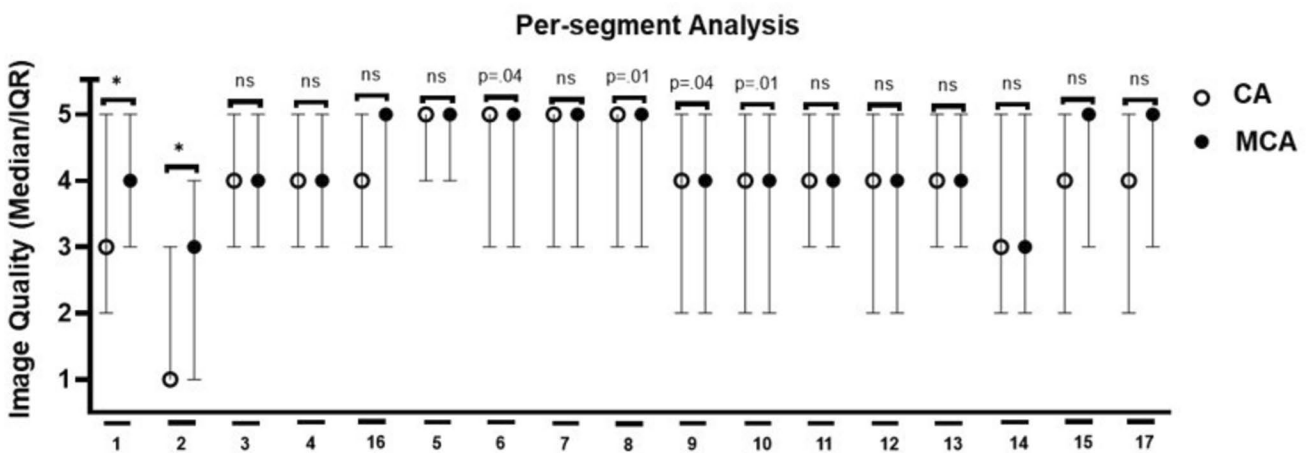

Fig. 3 Median and interquartile range of IQ per-segment with CA and MCA due to a 5-point Likert score. Significance is marked with an asterisk
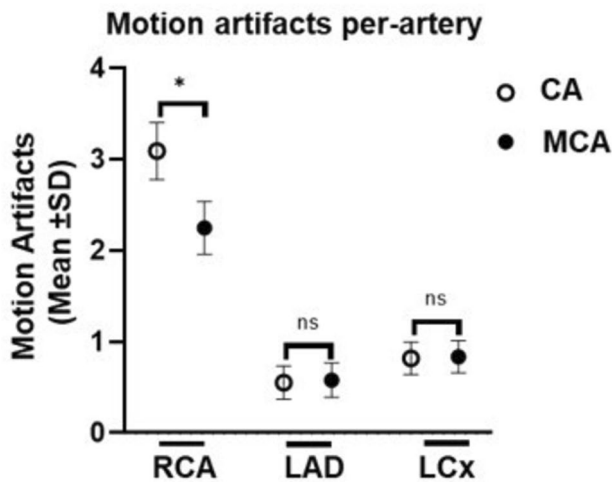
Fig. 4 Mean ± SD of motion artifacts per-artery. Significance is marked with an asterisk

reconstructed with both CA and MCA. There was no significant correlation between IQ and BMI, age, ΔHR, or sex.

Discussion

In this study, we evaluated the performance of a novel deep learning-based MCA by comparing IQ of 64-MDCT-acquired CCTA images. As in previous studies, the RCA and its segments 1 and 2 were found to be most prone to motion artifacts, as these are the most motile vessel segments [7]. MCA reconstruction had the greatest effect in these segments in improving IQ and reducing the total number of motion artifacts. Baseline IQ of LAD and LCx per-artery and

per-segment was initially much better; MCA-improvement of LAD and LCx was negligible. On the per-patient level, we observed an overall improvement of IQ. By evaluating potential disturbers, we found a significant negative correlation between mean HR and IQ for RCA, LAD, and LCx in CA- and MCA-reconstruction. However, the influence of mean HR was strong in the CA-reconstruction and intermediate in the MCA-reconstruction of the RCA. Correlation between mean HR and IQ of LAD and LCx was weak in both CA and MCA. BMI, age, sex, and ΔHR had no significant impact on IQ.

Recently, various MCA-based approaches have been published to mitigate motion artifacts. Two vendor-specific MCA are currently available (2023): SnapShot Freeze (SSF) 1 and its successor SSF2 (GE Healthcare, Waukasha, WI, USA) [13, 20]. In the clinical setting, SSF1 improved IQ and interpretability in ≥ 64-MDCT independent of HR and BMI [21, 22]. In addition, good IQ was maintained even at high HR, allowing wider application of PGI leading to a lower total effective dose [21, 23]. Therefore, SSF1 is considered a useful tool to assist CCTA in CCS diagnosis [12]. Positive effects of SSF2 on IQ are even more profound compared to its predecessor [13]. Unfortunately, both MCA are vendor-specific and only applicable on vendor-specific CT scanners [17]. Besides SSF1 and 2, there have been several attempts to develop even more effective and widely applicable MCA [11]. However, most of these suffer from limitations due to high effective dose, poor performance at high or irregular HR, or long computation time [11, 16, 24, 25]. The recently introduced deep learning-based MCA might be a solution. Deep learning-based MCA can be applied post-acquisitionally without the need for raw data [26]. By this, they have a very short computation time and can be
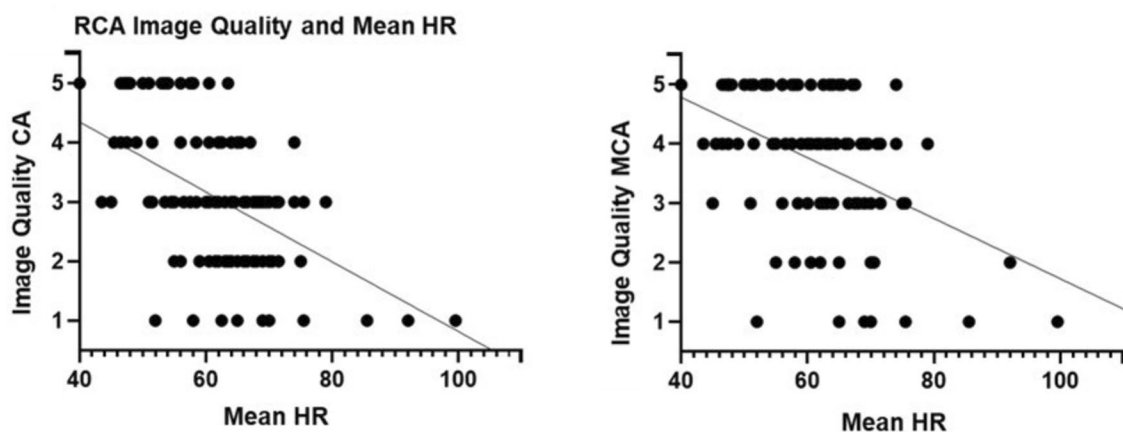

Fig. 5 Correlation (Spearman's Rho) of IQ improvement with CA and MCA due to a 5-point Likert score in the RCA and mean HR

used vendor-independently [11, 15]. However, larger studies on the performance of deep learning-based MCA are still scarce. Therefore, their clinical applicability cannot yet be assessed although phantom studies are promising [11, 15, 25].

In this study, we have found that the applied deep learning-based MCA *Deep PAMoCo* improves the IQ of 64-MDCT-acquired images [13, 15]. By this, the rate of non-diagnostic images and false-positive results could be remarkably reduced, especially at higher HR [22, 27, 28]. As CCTA is already considered to have a high-negative predictive value, this could further increase its validity for the diagnosis of CCS [1]. Especially regarding the limited temporal resolution of 64-MDCT, the presented MCA seems to be attractive to enhance 64-MDCT-acquired images. However, the applied MCA can also be expected to be useful in combination with high-end imaging technology, as high or irregular HR can also disturb $\geq$ 128-MDCT and DSCT imaging [29]. Besides IQ improvement, the tested MCA could also reduce the effective dose during CCTA, as PGI could be applied at higher HR, and by this more widely [21, 23]. However, as IQ still correlated with HR at an intermediate level, the presented MCA should be considered as a support and not as a substitute for HR control [30]. Finally, the tested MCA seems to be especially attractive in regard to its broad applicability due to its short computation time of 15s per entire CCTA image and its vendor-independent use [11, 15, 17]. Thus, the presented MCA resembles a low-effort software upgrade for CCTA imaging performed with a 64-MDCT.

This study has limitations. Firstly, since we wanted to test the ability of the MCA to compensate for motion artifacts and to improve IQ, patient data were not given in this trial. Secondly, in this study, we had to exclude eleven images completely and two partially because of stack transition, vessel calcifications, and medical devices (stents and pacemakers) producing massive artifacts. In addition, due to a lack of documentation, we were unable to determine BMI in 20 patients and mean HR, ΔHR, age, and sex in 9 patients. Thirdly, the evaluation of IQ was conducted by a sole professional. Consequently, we cannot provide an inter-observer agreement. Fourthly, the IQ assessment was conducted by employing a 5-point Likert score, consistent with previous research [19]. However, it is essential to note that there is no officially recommended approach for evaluating IQ, and therefore, the assessment lacks standardization. Consequently, the comparability with studies utilizing different assessment scores is restricted. Fifthly, the primary objective of this study was to evaluate the performance of the applied MCA in enhancing the IQ of real patient CCTA images. It is crucial to emphasize that the findings should not be generalized to other deep learning methods, given our limited study population and the focus on a sole MCA. Sixthly, this

was a single-center study. We recommend further studies at other radiology centers to increase the power and validity of our findings. Moreover, as this study aimed to evaluate the impact of a deep learning-based MCA on IQ, we cannot draw conclusions regarding its clinical utility. Further research is needed to evaluate the impact of MCA on diagnostic accuracy e.g. using invasive coronary angiography as a reference. Thus, it would also be possible to evaluate the impact of vessel calcification on IQ and MCA-related effective dose reduction. Finally, we did not compare the tested MCA with vendor-specific or other MCA. Thus, we cannot determine the superiority of the presented MCA.

Conclusion

In conclusion, this study has demonstrated on the one hand that the applied deep learning-based MCA is able to improve IQ in a large set of 64-MDCT-acquired real-patient images and, on the other hand, to reduce HR impact on IQ. Thus, the presented MCA can be considered as a promising example of deep learning-based MCA. Now, further studies should be done to evaluate the effectiveness of the presented MCA in regard to other MCA and to assess its clinical utility and diagnostic accuracy.

Abbreviations BMI: Body mass index; CA: Conventional algorithm; CCTA: Coronary computed tomography angiography; CCS: Chronic coronary syndrome; DSCT: Dual source computed tomography; ECG: Electrocardiogram; ESC: European society of cardiology; FOV: Field of view; HR: Heart rate; IQ: Image quality; i.v.: Intravenously; LAD: Left descending artery; LCx: Left circumflex artery; MCA: Motion correction algorithm; MDCT: Multidetector computed tomography; PGI: Prospective electrocardiographic-gated imaging; PTP: Pre-test probability; RBC: Rank-biserial correlation; RCA: Right coronary artery; SSF: SnapShot Freeze; ΔHR: Intra-cycle HR changes

Declarations

Ethics Approval Original image data were anonymised and patients are not identifiable. Human or animal subjects were not directly involved in this study.

Consent to Participate Original image data were anonymised and patients are not identifiable. Human or animal subjects were not directly involved in this study.

Consent for Publication Original image data were anonymised and patients are not identifiable. Human or animal subjects were not directly involved in this study.

Competing Interests The authors declare no competing interests.

Open Access This article is licensed under a Creative Commons Attribution 4.0 International License, which permits use, sharing, adaptation, distribution and reproduction in any medium or format, as long as you give appropriate credit to the original author(s) and the source, provide a link to the Creative Commons licence, and indicate if changes were made. The images or other third party material in this article are included in the article's Creative Commons licence, unless indicated otherwise in a credit line to the material. If material is not included in the article's Creative Commons licence and your intended use is not permitted by statutory regulation or exceeds the permitted use, you will need to obtain permission directly from the copyright holder. To view a copy of this licence, visit http://creativecommons.org/licenses/by/4.0/.

References

1. Knuuti J, Wijns W, Saraste A, et al. 2019 ESC Guidelines for the diagnosis and management of chronic coronary syndromes. *Eur Heart J*. 2020;41(3):407–477. https://doi.org/10.1093/eurheartj/ehz425

2. Narula J, Chandrashekhar Y, Ahmadi A, et al. SCCT 2021 Expert consensus document on coronary computed tomographic angiography: a report of the society of cardiovascular computed tomography. *J Cardiovasc Comput Tomogr*. 2021;15(3):192–217. https://doi.org/10.1016/j.jcct.2020.11.001.

3. Jiang B, Wang J, Lv X, Cai W. Dual-source CT versus single-source 64-section CT angiography for coronary artery disease: a meta-analysis. *Clin Radiol*. 2014;69(8):861–869. https://doi.org/10.1016/j.crad.2014.03.023

4. Hsiao EM, Rybicki FJ, Steigner M. CT coronary angiography: 256-slice and 320-detector row scanners. *Curr Cardiol Rep*. 2010;12(1):68–75. https://doi.org/10.1007/s11886-009-0075-z

5. Miller JM, Rochitte CE, Dewey M, et al. Diagnostic performance of coronary angiography by 64-row CT. *N Engl J Med*. 2008;359(22):2324–2336. https://doi.org/10.1056/NEJMoa0806576

6. Dekker MAM den, Smet K de, Bock GH de, Tio RA, Oudkerk M, Vliegenthart R. Diagnostic performance of coronary CT angiography for stenosis detection according to calcium score: systematic review and meta-analysis. *Eur Radiol*. 2012;22(12):2688–2698. https://doi.org/10.1007/s00330-012-2551-x

7. Husmann L, Leschka S, Desbiolles L, et al. Coronary artery motion and cardiac phases: dependency on heart rate -- implications for CT image reconstruction. *Radiology*. 2007;245(2):567–576. https://doi.org/10.1148/radiol.2451061791

8. Aghayev A, Murphy DJ, Keraliya AR, Steigner ML. Recent developments in the use of computed tomography scanners in coronary artery imaging. *Expert Rev Med Devices*. 2016;13(6):545–553. https://doi.org/10.1080/17434440.2016.1184968

9. Sun Z, Choo GH, Ng KH. Coronary CT angiography: current status and continuing challenges. *Br J Radiol*. 2012;85(1013):495–510. https://doi.org/10.1259/bjr/15296170

10. Graaf FR de, Schuijf JD, van Velzen JE, et al. Evaluation of contraindications and efficacy of oral Beta blockade before computed tomographic coronary angiography. *Am J Cardiol*. 2010;105(6):767–772. https://doi.org/10.1016/j.amjcard.2009.10.058

11. Lossau Née Elss T, Nickisch H, Wissel T, et al. Motion estimation and correction in cardiac CT angiography images using convolutional neural networks. *Comput Med Imaging Graph*. 2019;76:101640. https://doi.org/10.1016/j.compmedimag.2019.06.001

12. Lee H, Kim JA, Lee JS, Suh J, Paik SH, Park JS. Impact of a vendor-specific motion-correction algorithm on image quality, interpretability, and diagnostic performance of daily routine coronary CT angiography: influence of heart rate on the effect of motion-correction. *Int J Cardiovasc Imaging*. 2014;30(8):1603–1612. https://doi.org/10.1007/s10554-014-0499-4

13. Liang J, Sun Y, Ye Z, et al. Second-generation motion correction algorithm improves diagnostic accuracy of single-beat coronary CT angiography in patients with increased heart rate. *Eur Radiol*. 2019;29(8):4215–4227. https://doi.org/10.1007/s00330-018-5929-6

14. Deng F, Tie C, Zeng Y, et al. Correcting motion artifacts in coronary computed tomography angiography images using a dual-zone cycle generative adversarial network. *J Xray Sci Technol*. 2021;29(4):577–595. https://doi.org/10.3233/XST-210841

15. Maier J, Lebedev S, Erath J, et al. Deep learning-based coronary artery motion estimation and compensation for short-scan cardiac CT. *Med Phys*. 2021;48(7):3559–3571. https://doi.org/10.1002/mp.14927

16. Hahn J, Bruder H, Rohkohl C, et al. Motion compensation in the region of the coronary arteries based on partial angle reconstructions from short-scan CT data. *Med Phys*. 2017;44(11):5795–5813. https://doi.org/10.1002/mp.12514

17. Ren P, He Y, Zhu Y, et al. Motion artefact reduction in coronary CT angiography images with a deep learning method. *BMC Med Imaging*. 2022;22(1):184. https://doi.org/10.1186/s12880-022-00914-2

18. Leipsic J, Abbara S, Achenbach S, et al. SCCT guidelines for the interpretation and reporting of coronary CT angiography: a report of the Society of Cardiovascular Computed Tomography Guidelines Committee. *J Cardiovasc Comput Tomogr*. 2014;8(5):342–358. https://doi.org/10.1016/j.jcct.2014.07.003

19. Carrascosa P, Deviggiano A, Leipsic JA, et al. Dual energy imaging and intracycle motion correction for CT coronary angiography in patients with intermediate to high likelihood of coronary artery disease. *Clin Imaging*. 2015;39(6):1000–1005. https://doi.org/10.1016/j.clinimag.2015.07.023

20. Leipsic J, Labounty TM, Hague CJ, et al. Effect of a novel vendor-specific motion-correction algorithm on image quality and diagnostic accuracy in persons undergoing coronary CT angiography without rate-control medications. *J Cardiovasc Comput Tomogr*. 2012;6(3):164–171. https://doi.org/10.1016/j.jcct.2012.04.004

21. Machida H, Lin X-Z, Fukui R, et al. Influence of the motion correction algorithm on the quality and interpretability of images of single-source 64-detector coronary CT angiography among patients grouped by heart rate. *Jpn J Radiol*. 2015;33(2):84–93. https://doi.org/10.1007/s11604-014-0382-1

22. Fuchs TA, Stehli J, Dougoud S, et al. Impact of a new motion-correction algorithm on image quality of low-dose coronary CT angiography in patients with insufficient heart rate control. *Acad Radiol*. 2014;21(3):312–317. https://doi.org/10.1016/j.acra.2013.10.014

23. Li Z-N, Yin W-H, Lu B, et al. Improvement of image quality and diagnostic performance by an innovative motion-correction algorithm for prospectively ECG triggered coronary CT angiography. *PLoS One*. 2015;10(11):e0142796. https://doi.org/10.1371/journal.pone.0142796

24. Rohkohl C, Bruder H, Stierstorfer K, Flohr T. Improving best-phase image quality in cardiac CT by motion correction with

MAM optimization. *Med Phys*. 2013;40(3):31901. https://doi.org/10.1118/1.4789486

25. Kim S, Chang Y, Ra JB. Cardiac motion correction for helical CT scan with an ordinary pitch. *IEEE Trans Med Imaging*. 2018;37(7):1587–1596. https://doi.org/10.1109/TMI.2018.2817594

26. *2016 IEEE Conference on Computer Vision and Pattern Recognition (CVPR)*. IEEE; 2016.

27. Andreini D, Pontone G, Mushtaq S, et al. Low-dose CT coronary angiography with a novel IntraCycle motion-correction algorithm in patients with high heart rate or heart rate variability. *Eur Heart J Cardiovasc Imaging*. 2015;16(10):1093–1100. https://doi.org/10.1093/ehjci/jev033

28. Sun J, Okerlund D, Cao Y, et al. Further improving image quality of cardiovascular computed tomography angiography for children with high heart rates using second-generation motion correction algorithm. *J Comput Assist Tomogr*. 2020;44(5):790–795. https://doi.org/10.1097/RCT.0000000000001035

29. Liang J, Wang H, Xu L, et al. Impact of SSF on diagnostic performance of coronary computed tomography angiography within 1 heart beat in patients with high heart rate using a 256-row detector computed tomography. *J Comput Assist Tomogr*. 2018;42(1):54–61. https://doi.org/10.1097/RCT.0000000000000641

30. Sheta HM, Egstrup K, Husic M, Heinsen LJ, Nieman K, Lambrechtsen J. Impact of a motion correction algorithm on image quality in patients undergoing CT angiography: a randomized controlled trial. *Clin Imaging*. 2017;42:1–6. https://doi.org/10.1016/j.clinimag.2016.11.002